


Research Article

Candesartan restores blood–brain barrier dysfunction, mitigates aberrant gene expression, and extends lifespan in a knockin mouse model of epileptogenesis

 Michael F. Hammer^{1,2}, Erfan Bahramnejad^{1,3}, Joseph C. Watkins⁴ and Patrick T. Ronaldson³

¹BIO5 Institute, University of Arizona, Tucson, AZ, U.S.A.; ²Department of Neurology, University of Arizona, Tucson, AZ, U.S.A.; ³Department of Pharmacology, University of Arizona, Tucson, AZ, U.S.A.; ⁴Department of Mathematics, University of Arizona, Tucson, AZ, U.S.A.

Correspondence: Michael F. Hammer (mfh@email.arizona.edu)



Blockade of Angiotensin type 1 receptor (AT1R) has potential therapeutic utility in the treatment of numerous detrimental consequences of epileptogenesis, including oxidative stress, neuroinflammation, and blood–brain barrier (BBB) dysfunction. We have recently shown that many of these pathological processes play a critical role in seizure onset and propagation in the *Scn8a-N1768D* mouse model. Here we investigate the efficacy and potential mechanism(s) of action of candesartan (CND), an FDA-approved angiotensin receptor blocker (ARB) indicated for hypertension, in improving outcomes in this model of pediatric epilepsy. We compared length of lifespan, seizure frequency, and BBB permeability in juvenile (D/D) and adult (D/+) mice treated with CND at times after seizure onset. We performed RNAseq on hippocampal tissue to quantify differences in genome-wide patterns of transcript abundance and inferred beneficial and detrimental effects of canonical pathways identified by enrichment methods in untreated and treated mice. Our results demonstrate that treatment with CND gives rise to increased survival, longer periods of seizure freedom, and diminished BBB permeability. CND treatment also partially reversed or ‘normalized’ disease-induced genome-wide gene expression profiles associated with inhibition of NF- κ B, TNF α , IL-6, and TGF- β signaling in juvenile and adult mice. Pathway analyses reveal that efficacy of CND is due to its known dual mechanism of action as both an AT1R antagonist and a PPAR γ agonist. The robust effectiveness of CND across ages, sexes and mouse strains is a positive indication for its translation to humans and its suitability of use for clinical trials in children with *SCN8A* epilepsy.

Introduction

Epilepsy is a common neurological disorder that can have devastating consequences for children [1]. Advances in genomic research have implicated many individually rare genetic variants as causal for a significant proportion of early-onset epilepsy [2]. Pathogenic gain-of-function variants in the voltage-gated sodium channel gene, *SCN8A*, underlie a severe early onset seizure syndrome that is accompanied by global developmental delays, intellectual disabilities, and a host of comorbidities [3]. These variants alter the function of the Na ν 1.6 channel, the most abundant sodium channel in the human brain and a master regulator of neuronal excitability [4]. Unfortunately, more than 75% of *SCN8A* patients treated with

Received: 23 April 2024
Revised: 01 August 2024
Accepted: 02 August 2024

Accepted Manuscript online:
02 August 2024
Version of Record published:
03 September 2024

currently marketed antiseizure medications (ASM) do not achieve seizure freedom, and many suffer adverse side effects. Indeed, there are no commercially available drugs that specifically target SCN8A or that prevent progression of the disease [5].

We previously investigated a mouse model with a pathogenic *Scn8a* knockin variant (N1768D) and found that prior to seizure onset there was increased blood–brain barrier (BBB) permeability and genome-wide alterations in transcript abundance, both of which were exacerbated once seizures were established [6]. These patterns of disease progression fit a model of epileptogenesis (i.e., the process by which neuronal networks are altered toward increased seizure susceptibility and generation of chronic spontaneous seizures), similar to that seen in post-traumatic epilepsy in which there is an initial injury, a latent phase and a chronic epilepsy phase [7]. We suggested that pathological conditions associated with SCN8A-related epilepsy include the same pathogenic ‘tetrad’ of glutamate excitotoxicity, oxidative stress (OXS), inflammation, and BBB dysfunction (BBBD) that characterizes the neurobiology of other brain disorders [6,8].

Angiotensin receptor blockers (ARBs) represent a class of drugs that has shown promise in treating the ‘injury cascade’ associated with brain insults by effectively blocking the physiological effects of angiotensin II, the main active factor of the renin–angiotensin system (RAS) [9]. After brain injury, and in various brain disorders, increased Angiotensin II (Ang II) activates the Angiotensin type 1 receptor (AT1R) leading to glutamate excitotoxicity, OXS, BBB breakdown, brain inflammation, cerebrovascular remodeling, as well as other risk factors for neuronal injury, cognitive decline, post-traumatic epilepsy, and neurodegenerative diseases [10,11]. Blocking AT1R activation with ARBs has therapeutic potential in many chronic disease states [11,12] as they are known to have powerful anti-inflammatory, anti-fibrotic, and antioxidant activities [11,13,14]. In addition, some studies have shown promising effects in various epilepsy models [15–19]. Therefore, blocking AT1R activation with ARBs has therapeutic potential in many chronic disease states [11,12].

In this study, we test the efficacy of candesartan (CND), an FDA-approved ARB indicated for hypertension, for its ability to prevent BBB dysfunction and mitigate epileptogenesis in our *Scn8a* mouse model, which includes the N1768D variant in heterozygous (D/+) and homozygous (D/D) form on two strain backgrounds (C57BL/6J and C3H/HeJ). In particular, we examine survival and seizure frequency in untreated and treated juveniles, as well as in untreated and treated adults of both sexes and on both strain backgrounds. We carry out BBB permeability studies and RNAseq on hippocampal tissues in order to determine (1) what distinguishes gene expression signatures of untreated and treated juveniles and adults, (2) which pathways are altered in a manner consistent with overstimulation of AT1R, and (3) by what mechanism(s) CND treatment leads to improved outcomes.

Materials and methods

Mouse strains

The C57BL/6J-N1768D congenic mouse (B6-D/+) was used for phenotyping, RNAseq and BBB studies [20]. In addition, a hybrid strain that was produced by backcross breeding to transfer the *Scn8a*-N1768D allele from the B6 to the C3H/HeJ strain background was used to further assess the effect of CND on survival and seizure frequency. After constructing an F1 by crossing male B6-D/+ heterozygotes to female C3H/HeJ, five rounds of backcrossing (N6) produced a 2.5% B6 and 98.5% C3H/HeJ-N1768D line (C3H-D/+). Sister-brother mating maintained the 98.5% C3H background. This line (referred to here as C3H) was observed to have an altered phenotype in terms of survival of the homozygote (C3H-D/D), which typically only survive for ~25 days after a series of ~60–80 tonic-clonic seizures (TCs) beginning at ~15–20 days of age (Figure 1A). C3H-D/D mice have a delayed seizure onset (~40–45 days) and an extended survival (65–70 days) with intermittent bouts of TCs (Figure 1A).

Phenotyping

Female and male mice on both the B6 and C3H backgrounds were housed in sex-specific groups of 3–4 per cage in a pathogen-free mouse facility with a 14 h light/10 h dark cycle (lights turned on at 5am). As described previously [6], a 24/7 video monitoring system was utilized to collect seizure data, with infrared illumination to monitor behavior during the dark period. Seizures were counted as individual TCs as described in [6,20]. Adult mice were followed from the age of 6 weeks, a period of time well before seizure onset, in order to identify the day of seizure onset. We define a seizure bout as a cluster of seizures on consecutive days, and a gap as a seizure-free period of 3 days or more [6]. This research received formal approval from the University of Arizona Institutional Animal Care and Use Committee Program (IACUC #16-160). All experiments were designed in accordance with the Animal Research: Reporting In Vivo Experiments (ARRIVE) guidelines [21] and efforts were made to minimize animal stress and suffering and to

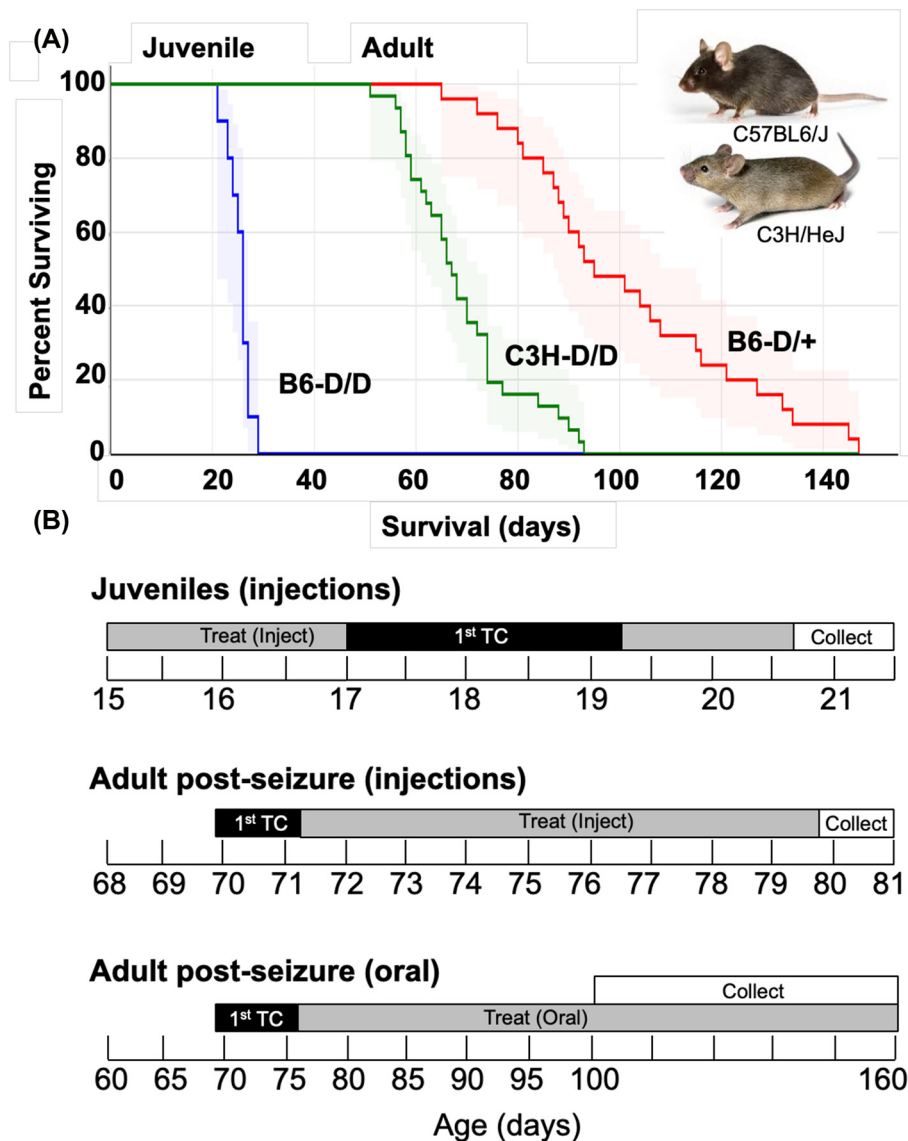


Figure 1. Mouse lines and dosing regimen for B6-D/D juvenile and B6-D/+ adult mice

(A) Survival curves for three mouse lines under study. Seizure onset for B6-D/+ heterozygotes is at ~75 days and survival declines to near 0% between 80 and 140 days, seizure onset for B6-D/D homozygotes is at ~15–20 days and survival declines to near 0% between 21 and 28 days, and seizure onset for C3H-D/D mice begins ~40–45 days and survival declines to near 0% between 60 and 90 days. (B) Black bars indicate approximate seizure onset times for B6-D/D juveniles and B6-D adults. Treatment by injection or by oral dosing starts on day after first seizure for adults (shown in gray bars). There is a daily subcutaneous (s.c.) injection over 5 days for juveniles and a 10-day series for adults starting at seizure onset. Oral dosing for adults starts at seizure onset and continues for an extended period before collection, which corresponds to age for VEH-treated mice to experience ~20 TCs.

reduce the number of mice used. Genotyping at the Scn8a-N1768D site was carried out as previously described [6,20]

Drug administration

Preparation of CND suspension for injections and oral dosing

Juvenile B6-D/D and adult B6-D/+ mice were given subcutaneous (s.c.) injections with either CND (2–4 mg/kg/day; doses that fall within the FDA-approved range for CND in both adults and children) or vehicle (VEH) (Sigma-Aldrich) [22,23] (Figure 1B). Oral dosing of adults was performed by thoroughly mixing 160 µl of suspension containing 1.28 mg of CND or VEH with 5 g of pure (organic) peanut butter in a petri dish [20]. Mice were given 1 g

pellet per mouse each day. Pellets were weighed each day to record amount consumed and 24/7 video used to verify that each mouse was consuming pellet. An average of 0.79 g (± 0.36 g) was consumed by an adult mouse (~ 20 – 25 g), corresponding to 9.1 ± 4.2 mg/kg/day. No correlations were found for amount of CND consumed and lifetime survival or number of TCs (Supplementary Figure S1).

Survival and seizure frequency studies

B6-D/D mice were injected with CND ($n=10$) or VEH ($n=10$) at 15 days of age (P15) and followed to monitor TCs by 24/7 video recording until death (Figure 1B). A separate set of 10 B6-D/D mice was administered a daily s.c. injection of 25 mg/kg/day phenytoin (PHT) suspension or VEH (US Pharmacopeia, Sigma-Aldrich) [24]. Oral administration of CND or VEH was initiated at the time of seizure onset (range P75–P85) for adult B6-D/+ females ($N=10$) and males ($N=10$) (Figure 1B). Mice were monitored for seizures by 24/7 video recording until time of death.

Transcriptome studies

B6-D/D and wild-type (+/+) ($n=3$) were administered CND or VEH by s.c. injection for a period of 5 days starting at P15 and sacrificed for removal of hippocampal tissue ($n=12$) (Figure 1B). Adult B6-D/+ male ($n=3$) mice were administered CND or VEH pellets as described above at the time of seizure onset and monitored for seizures for an extended period before sacrifice and removal of hippocampal tissue (100–160 d) (i.e., to match the age at which a VEH-treated male B6-D/+ experience ~ 20 TCs) (Figure 1B).

Blood–brain barrier studies

B6-D/+ females ($n=6$) and males ($n=6$) were administered CND (2–4 mg/kg/day) or VEH by s.c. injection at the time of seizure onset for a period of 10 days (Figure 1B). On the 11th day these two groups of mice were subjected to BBB analysis as described in the next section.

Blood–brain barrier analysis

Changes in BBB integrity were assessed by enhanced brain accumulation of ^{14}C -sucrose (PerkinElmer Life and Analytical Sciences, Boston, MA). *In situ* perfusion with radiolabeled sucrose was performed as previously described [6,25–27]. Briefly, mice were anesthetized with ketamine/xylazine and heparinized to ensure anticoagulation. An incision was made in the neck and the right carotid artery was exposed and cannulated. Following cannula placement, the mouse was perfused with an artificial plasma solution warmed to 37°C and continuously oxygenated containing [^{14}C]sucrose (Specific Activity = 0.5 mCi/ml) delivered via a slow-drive syringe pump. After 10 min of perfusion, the cannulae was removed and the animal was decapitated. The brain was rapidly removed and cerebral hemispheres were sectioned. Radioactivity of [^{14}C]sucrose was measured by liquid scintillation counting. Results were reported as picomoles of radiolabeled sucrose per milligram of brain tissue (R_{Br}; pmol/mg tissue), which is equal to the total amount of ^{14}C -sucrose in the brain (R_{Brain}; dpm/mg tissue) divided by the amount of radioisotope in the perfusate (R_{Perfusate}; dpm/pmol) (eqn 1):

$$\text{RBr} = \frac{\text{R}_{\text{Brain}}}{\text{R}_{\text{Perfusate}}} \quad (1)$$

RNA sequencing

Hippocampal tissues from 21 mice were obtained according to a sampling strategy that compared (1) untreated (VEH only) and treated B6-D/D ($n=3$) with age-matched B6-+/+ controls ($n = 3$ per group), (2) untreated (VEH only) male B6-D/+ mice that had experienced ~ 20 TCs ($n = 3$ per group) with age-matched B6-+/+ controls ($n = 3$ per group), and (3) male B6-D/+ mice that were treated with CND for an extended period ($n = 3$ per group). Brains of treated and untreated mice were dissected to yield tissue samples from the hippocampus [28]. Bulk tissue was stored in RNALater (Qiagen, Valencia, CA) at -80 degrees centigrade. The technique for analyzing hippocampal gene expression was performed as previously described [6]. Briefly, RNA was isolated from hippocampal tissue and initial QC performed. Libraries were constructed using a stranded mRNA-Seq Kit and average fragment size was assessed. After concentrations were determined with an adaptor-specific qPCR kit, equimolar samples were pooled and clustered for sequencing on a Novaseq instrument (Illumina). Sample data were demultiplexed, trimmed and quality filtered, and Fastq files were splice aligned against the GRCh37 reference genome using STAR aligner version 2.5.2b [29]. Gene expression counts were obtained using htseq-count version 0.6.1 [30]. Both splice alignment and counting were performed with Ensembl Annotation of the NCBI reference genome and raw counts analyzed with edgeR version 3.16.5 [31].

Data and pathway analysis

Results of statistical summaries were generally expressed as mean \pm SD. Kaplan–Meier survival curves were used to test for differences in survival. In cases where groups did not have the same variance, we performed two-sample *t*-tests. We used a ‘perturbation signature’ approach to identify genome-wide differences in transcript abundance between transgenic mice (i.e., D/+, D/D or +/+) that were untreated (VEH) or treated with CND [32]. Differential expression analysis was performed as previously described [33,34]. Briefly, we utilized the exactTest function in edgeR and gene expression counts were first normalized using the calcNormFactors function. DEG analysis was performed on treatment versus control groups at two different ages using three biological replicates per group, which has been shown in power analyses to be sufficient to yield a true positive rate greater than 80% under the conditions used here [35]. Multidimensional scaling (MDS) plots were constructed using the ‘plotMDS’ function in edgeR, which plots samples on a 2D scatterplot so that distances on the plot approximate the typical log₂ fold changes between samples. All significant differentially expressed genes (DEGs) (false discovery rate [FDR] < 0.05) were analyzed with Ingenuity[®] Pathway Analysis (IPA) to identify biological pathways that were significantly activated or deactivated as compared with controls and to identify putative upstream transcriptional regulators (Qiagen, Hilden, Germany). Rather than focusing on any single gene, bioinformatic analyses of our RNAseq data identified the most statistically significant biological pathways that were enriched given the set of DEGs in each experiment.

Pathway literature searches and feature selection

ChatGTP was used to aid in literature searches on the role of canonical pathways identified by IPA in the context of brain disorders. Initially, the question was posed: ‘what does “canonical pathway name” have to do with brain injury?’ Several pathway ‘effects’ commonly reported in pathological conditions (e.g., neuroinflammation, BBB, etc.) were identified in the untreated and treated B6-D/D juvenile and B6-D/+ male adults. A second round of searches was performed including the term ‘activation’ or ‘deactivation’; for example, ‘what does activation/deactivation of the “canonical pathway” name have to do with brain injury?’ For each canonical pathway, a score of 1 or 2 was assigned to each effect depending on whether it was ‘detrimental’ or ‘beneficial’, respectively, in association with an activated or deactivated state as appropriate. For example, in the case of the pathway effect ‘neuroinflammation’, a ‘1’ or ‘2’ was assigned if pro- or anti-inflammatory cytokines were inferred to be produced early and/or late in the injury process, respectively. A score of 1/2 was assigned if the effect was beneficial in one context and detrimental in another. If an effect was not involved in a given pathway it was assigned ‘0’. An underlying assumption in the interpretation of whether an effect was beneficial or detrimental was that mice were sampled in the later stages of epileptogenesis (i.e., after the establishment of spontaneous seizures) [6]. Finally, a list of cited references in each search was compiled and inspected to verify results for the pathways that were deemed to be most relevant in the study.

Results

Differential survival and seizure frequency for untreated and treated mice Adults

Supplementary Table S1 displays survival and seizure statistics for female and male untreated (*N*=17) and treated (*n*=10) B6-D/+ monitored 24/7 by video beginning at P30 and continuing for the remainder of their entire life span. Data for the untreated mice were previously reported [6]. Supplementary Table S1 also provides C3H-D/D summary statistics for female untreated (*N*=15) and treated (*N*=15) and male untreated (*N*=27) and treated (*N*=16) monitored until time of death. Age at seizure onset was not significantly different for untreated and treated mice within each line, except in the case of male C3H-D/D (44.0 \pm 6.5 days vs 48.1 \pm 5.1 days, *t*-test *P*-value = 0.018).

In all cases, treated mice lived longer and experienced a lower post-onset seizure frequency. For example, there was a significant increase in survival of B6-D/+ treated versus untreated females (167.6 \pm 19.1 vs 132.9 \pm 21.4 days, *t*-test *P*-value = 1.38 \times 10⁻⁴) and B6-D/+ treated versus untreated males (135.8 \pm 28.4 vs 91.3 \pm 15.2 days, *t*-test *P*-value = <1.0 \times 10⁻⁵), reflecting a 34.7% and 48.9% increase, respectively (Figure 2A and Supplementary Table S1). Similarly, C3H-D/D treated versus untreated females (69.9 \pm 12.9 vs 117.4 \pm 28.0 days, *t*-test *P*-value = <1.0 \times 10⁻⁵) and C3H-D/D treated versus untreated males (67.9 \pm 9.9 vs 117.1 \pm 20.4 days, *t*-test *P*-value = <1.0 \times 10⁻⁵), reflecting a 47.5% and 49.2% increase, respectively (Supplementary Figure S2 and Table S1).

Kaplan–Meier survival curves are shown for all adults in Supplementary Figure S3 and for C3H-D/D in Figure 2B. Unequal survival of treated versus untreated B6-D/+ females and males was strongly supported in a goodness of fit test using the χ^2 distribution (right-tailed) (*P*-value = 2.1 \times 10⁻³ and 3.5 \times 10⁻⁴, respectively), which also indicated a medium and large observed standard effect sizes of 0.59 and 0.69, respectively (Supplementary Figure S3A and S3B). C3H-D/D treated females and males showed similar patterns, with unequal survival strongly supported (*P*-values =

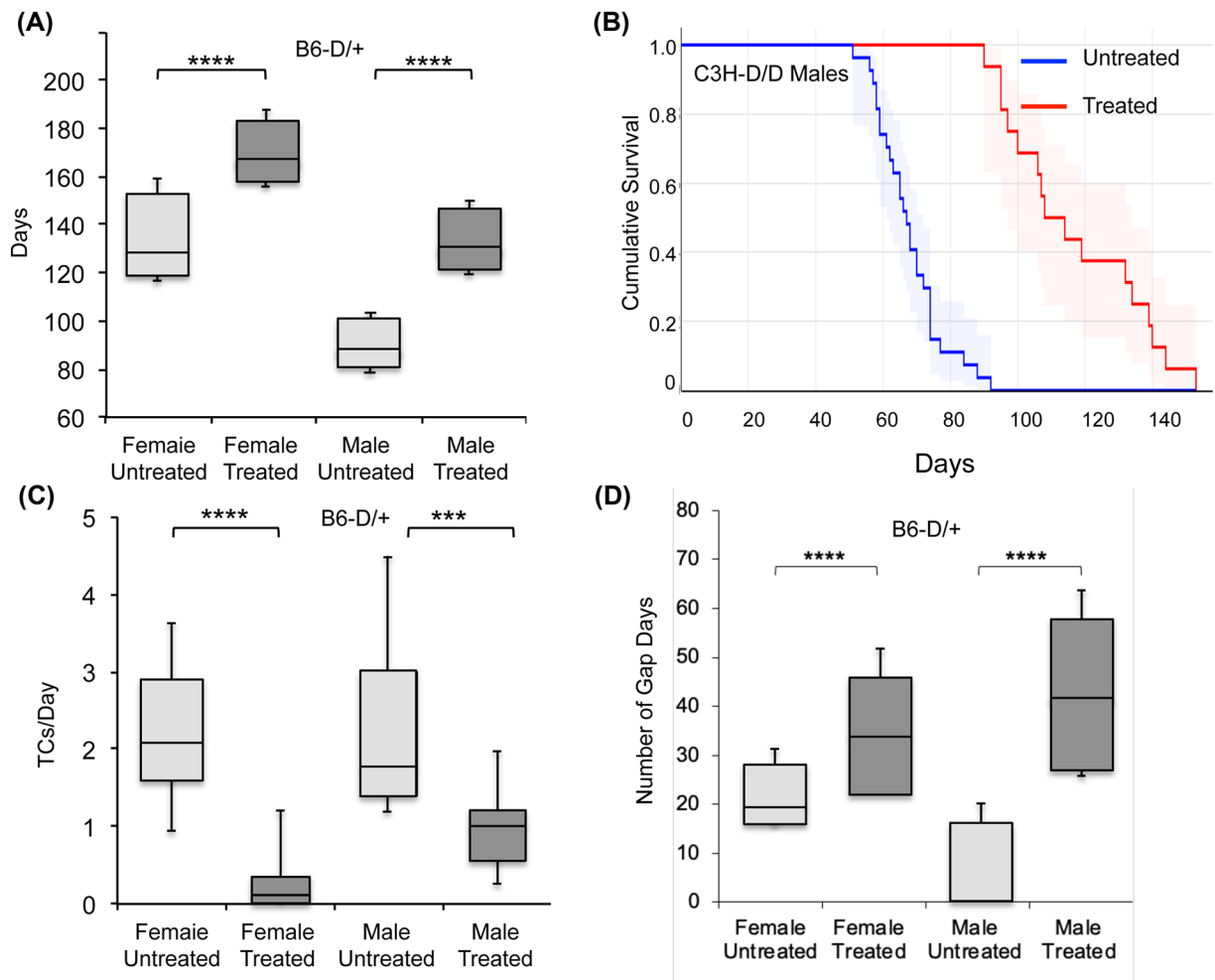


Figure 2. Lifetime survival, seizure frequency and seizure gaps for adult mice

Boxplots showing (A) lifetime survival for untreated and treated B6-D/+ females and males. (B) Kaplan–Meier survival curves for untreated (blue) and treated (red) C3H-D/D male adults. Log rank test P -value 2.15×10^{-7} , standardized effect size = 0.79. (C) Boxplots for post seizure onset seizure frequencies for untreated (VEH only) and treated B6-D/+ female and male adults. (D) Boxplots showing number of seizure-free days between seizure bouts for untreated and treated B6-D/+ female and male adults ($*P < 0.05$, $**P < 0.01$, $***P < 0.001$, $****P < 0.0001$; ns = not significant).

$< 1.0 \times 10^{-5}$ in both cases) with large observed standard effect sizes of 0.83 (supplementary Figure S3C) and 0.79, respectively (Figure 2B).

Treated adult mice also had a lower post-onset seizure frequency, with B6-D/+ females and males experiencing 88.9% and 59.1% reductions, respectively (t -test P -value = $< 1.0 \times 10^{-5}$ and 9.4×10^{-4} , respectively) (Figure 2C); and C3H-D/D females and males experiencing 78.4% and 48.0% reductions, respectively (t -test P -value = 4.2×10^{-2} and = 1.2×10^{-4} , respectively) (Supplementary Figure S2D and Table S1). These reductions are reflected in a greater number of post-onset seizure gaps (i.e., ≥ 3 seizure-free days) [6] for B6-D/+ males (t -test P -value = 3.9×10^{-2}) and C3H-D/D females (t -test P -value = $< 1.0 \times 10^{-5}$) and males (t -test P -value = $< 1.0 \times 10^{-5}$) (Supplementary Figure S4 and Table S1). In addition, there was a greater gap length in B6-D/+ females (t -test P -value = 1.6×10^{-4}) and males (t -test P -value = 3.6×10^{-5}), as well as in C3H-D/D males (t -test P -value = 3.3×10^{-2}) (Supplementary Figure S3 and Table S1), resulting in a greater number of ‘gap days’ (shown for B6-D/+ in Figure 2D).

Juveniles

Supplementary Table S2 displays survival and seizure statistics for two groups of untreated and treated B6-D/D juvenile mice: a set treated with CND ($N=10$) and VEH ($N=10$) and a second set treated with PHT ($N=10$) and VEH

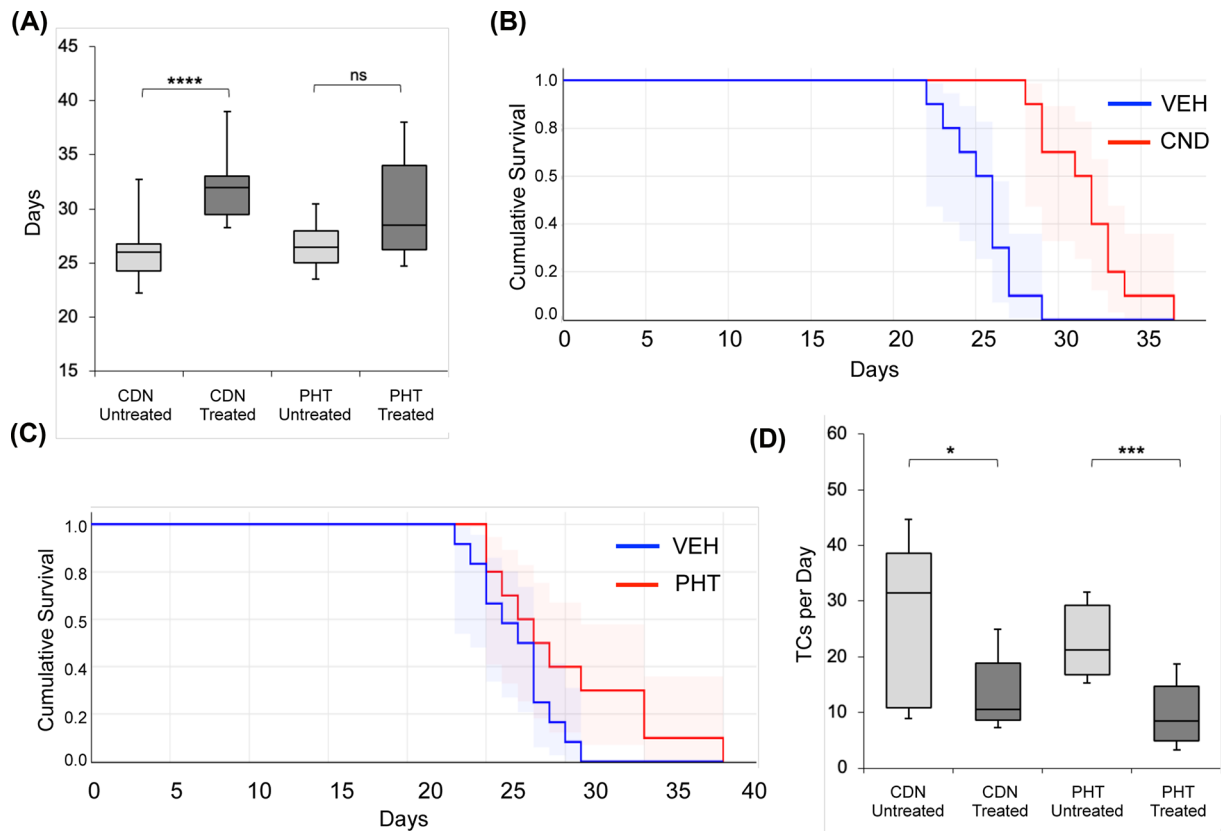


Figure 3. Lifetime survival and seizure frequency for juveniles treated with CDN and PHT

(A) Boxplots showing lifetime survival for juveniles treated with CDN and PHT compared with untreated (VEH only) controls. (B) Kaplan–Meier survival curves for B6-D/D juveniles treated with CDN (red) compared with untreated (VEH only) controls (blue). Log rank test P -value 4.2×10^{-5} , standardized effect size = 0.79. (C) Kaplan–Meier survival curves for B6-D/D juveniles treated with PHT (red) compared with untreated (VEH only) controls (blue). Log rank test P -value 0.132 (* $P < 0.05$, ** $P < 0.01$, *** $P < 0.001$, **** $P < 0.0001$; ns = not significant). (D) Boxplots showing post-onset seizure frequency for juveniles treated with CDN and PHT compared with untreated (VEH only) controls.

($N=10$). There was a significant increase (27%) in survival of juveniles treated with CDN (31.8 ± 2.7 vs 25.5 ± 2.1 days, t -test P -value = $< 1.0 \times 10^{-5}$) (Figure 3A; Supplementary Table S2). Juveniles treated with PHT experienced a minor increase in survival that did not reach statistical significance (30.1 ± 5.1 days vs 27.6 ± 3.2) (t -test, P -value = 0.083). Kaplan–Meier survival curves similarly show unequal survival of CDN treated versus untreated juveniles (P -value = 4.2×10^{-5}) with a large observed standard effect sizes of 0.79 (Figure 3B), while PHT treated juveniles did not show a statistically significant increase in survival (P -value = 0.132) (Figure 3C). For juveniles treated with CDN there was a slight decrease in post-onset seizure frequency (15.4 ± 10.3 vs 28.4 ± 17.7 TCs, t -test, P -value = 2.9×10^{-2}), and a more robust reduction in post-onset seizure frequency for juveniles treated with PHT (10.2 ± 7.1 vs 24.8 ± 11.0 TCs, t -test, P -value = 7.4×10^{-4}) (Figure 3D; Supplementary Table S2).

Effect of CDN on blood–brain barrier permeability in female and male adults

Our results previously demonstrated that BBB paracellular permeability (i.e., ‘leak’) to [^{14}C]sucrose, a small molecule tracer that does not cross the intact BBB [36], increased in both pre-TC B6-D/+ females and males relative to wild-type controls [6]. The magnitude of the sucrose permeability increase was shown to further increase over wild-type and pre-seizure levels in untreated post-TC B6-D/+ females and males. Treatment with CDN before seizure onset prevents BBB paracellular permeability from increasing above physiological levels in both B6-D/+ females and males

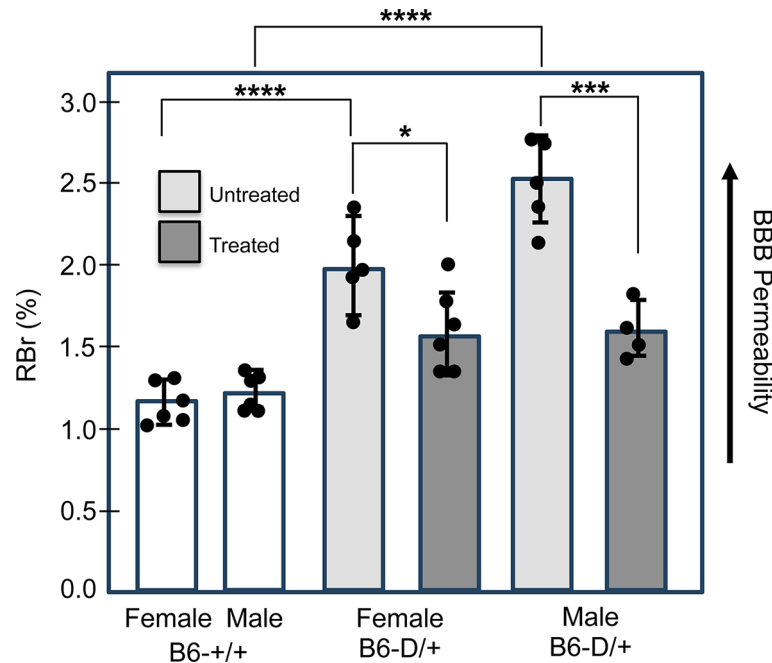


Figure 4. BBB paracellular permeability to sucrose is increased in untreated B6-D/+ female and male mice relative to those treated with CND after seizure activity

In situ brain perfusion with ¹⁴C-sucrose as a vascular permeability marker shows significantly elevated radioactivity represented by brain-to-perfusate radioactivity ratios (RBr %) in brains of untreated (VEH only) mice (light gray fill) after detection of seizures and compared with that of control (+/+) mice (white fill bar) and mice treated with CND (dark gray fill). Data are expressed as mean ± SD of 5–6 animals per treatment group (**P*<0.05, ***P*<0.01, ****P*<0.001, *****P*<0.0001; ns = not significant).

(data not shown). After seizure onset, treatment with CND results in a statistically significantly reduced BBB paracellular permeability (i.e., ‘leak’) relative to untreated post-seizure females (*P*<0.05) and untreated post-seizure males (*P*<0.001) (Figure 4).

Effects of CND on hippocampal gene expression in juvenile and adult mice

Figure 5A shows an MDS plot of the 500 most variably expressed genes for the 21 B6-D/D and B6-D/+ individuals submitted to RNAseq analysis. The plot shows untreated juveniles and adults on the left side of the plot and CND-treated juveniles and adults clustering on the right side with age-matched wild-type individuals. The co-clustering of juvenile and adult mice on both sides of the plot suggests that treatment with CND is the chief explanatory factor (i.e., more important than age or genotype) underlying inter-group genome-wide gene expression differences.

To further investigate the effects of CND treatment on gene expression in mice experiencing TCs, we characterized the number of DEGs that are up-regulated and down-regulated in the untreated and treated groups. For untreated juveniles, 1518 transcripts were identified with an FDR-adjusted *P*-value <0.05, 956 of which were up-regulated and 562 of which were down-regulated (Figure 5B, upper panel). CND-treated B6-D/D mice had a much smaller number of DEGs: 50 up-regulated and 25 down-regulated. Only 6 of the up-regulated and 2 of the down-regulated transcripts were shared with untreated mice. Untreated B6-D/+ adult males had a total of 602 DEGs (FDR-adjusted *P*-value <0.05), 454 of which were up-regulated and 148 were down-regulated. CND-treated B6-D/+ males had 86 DEGs: 76 up-regulated and 10 down-regulated. Four upregulated transcripts were shared between untreated and treated males (Figure 5B, upper panel).

Canonical pathways altered in untreated and treated juvenile mice

For untreated B6-D/D juveniles, pathway enrichment procedures identified 52 canonical pathways with *P*-values ≤0.05 and z-scores with absolute values ≥2.0 (Supplementary Table S3), including 10 predicted to be deactivated and 42 predicted to be activated (Figure 5B, lower panel). There were no enriched canonical pathways for CND-treated

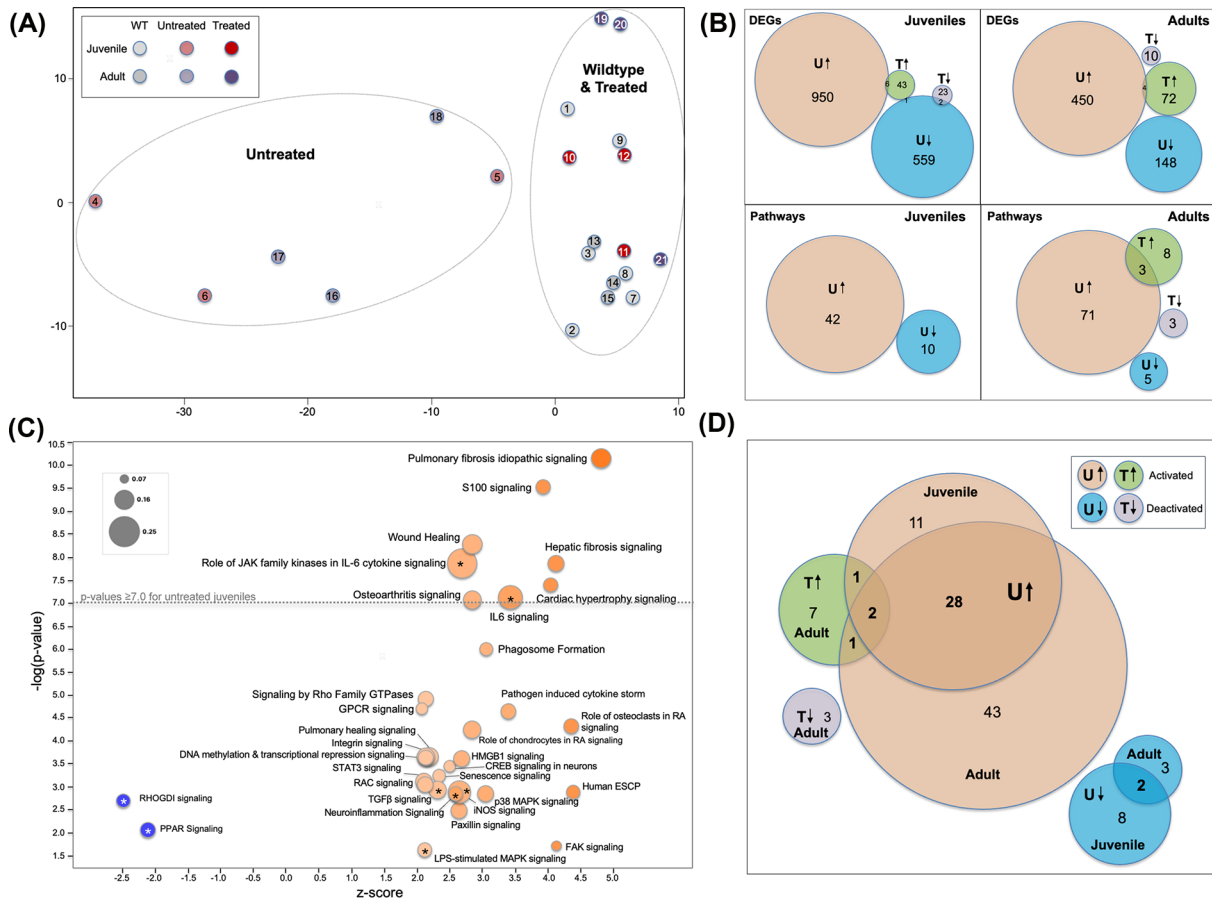


Figure 5. Number of differentially expressed genes and pathways identified by RNAseq and pathway enrichment analysis for untreated and treated B6-D/D juvenile and B6-D/+ adult mice

(A) MDS plot of 500 most variable genes in untreated (lighter purple and red fill) and treated (darker purple and red fill) B6-D/D juveniles and B6-D/+ adult males, as well as age-matched controls (B6-+/+) (gray-scale fill). Individuals of each type are represented by gray scale fill. Correspondence between numbers in circles and mouse phenotype and treatment status are shown in Supplementary Table S5. **(B)** Number of DEGs (DEGs) identified in B6-D/D juveniles (top left) and B6-D/+ adult males (top right); (blue: down-regulated, salmon: up-regulated) and treated (mauve: down-regulated, green: up-regulated). Number of significantly enriched canonical pathways identified by IPA in B6-D/D juveniles (bottom left) and B6-D/+ adult males (bottom right); (blue: deactivated, salmon: activated) and treated (mauve: down-regulated, green: up-regulated). **(C)** Bubble charts showing significantly enriched pathways ($-\log(P\text{-value}) \geq 1.3$) shared by B6-D/D juveniles and B6-D/+ adult males, color-coded by strength of activation (positive z-score $\geq +2.0$) or deactivation (negative z-score ≤ -2.0). Asterisks indicate most detrimental pathways (i.e., ≥ 6 detrimental effects, Supplementary Table S3). **(D)** Venn diagram showing number of canonical pathways shared or unique to untreated and treated B6-D/D juveniles and B6-D/+ adult males. Color scheme same as in (B).

B6-D/D under strict FDR. After relaxing the FDR cutoff from 0.05 to 0.25 a set of related pathways became statistically significant in treated juveniles: Oxidative Phosphorylation ($-\log(P\text{-value}) = 9.9$, z-score = 5.0), EIF2 Signaling ($-\log(P\text{-value}) = 4.2$, z-score = 3.2), Mitochondrial Dysfunction ($-\log(P\text{-value}) = 7.6$, z-score = -3.8), and Granzyme A Signaling ($-\log(P\text{-value}) = 5.5$, z-score = -3.4). The enrichment results reflect a common set of 19 up-regulated electron transport chain (ETC) subunit genes that alternately result in positive and negative activation z-scores for the oxidative phosphorylation (OXPHOS) and mitochondrial dysfunction (MD) pathways, respectively (another 24 non-ETC genes distinguish the MD from OXPHOS pathways). These genes include 12 within ETC complex I (Ndufa2, Ndufa4, Ndufa6, Ndubf4, Ndubf6, Ndufs3, Ndufs4, Ndufs6, Ndufs7, Ndufs8, Ndufv1, and Ndufv2), 3 within ETC complex III (Uqcrc1, Uqcr2 and Uqcr11), and 4 within ETC complex IV (Cox6c, Cox7a2, Cox7b, and Surf1). Only a single transcript out of 96 ETC genes was differentially expressed in untreated juveniles; the up-regulation of UCP2 (+3.32-fold, $P\text{-value} = 1.39 \times 10^{-8}$, z-score = 1.06×10^{-5}) has been shown to shift metabolism away from

OXPPOS toward glycolysis [37]. A Fisher exact test comparing the number of differentially expressed ETC genes (FDR ≤ 0.25) in treated versus untreated yields a P -value of 1.64×10^{-5} , and results in an odds ratio representing a 23-fold enhancement of ETC gene activation in treated juveniles (95%CI = 3.5–979).

Canonical pathways altered in untreated and treated adult mice

For untreated B6-D/+ adults, pathway enrichment procedures identified 79 canonical pathways with P -values ≤ 0.05 and z -scores with absolute values ≥ 2.0 (Supplementary Table S3), including 5 predicted to be deactivated and 74 predicted to be activated (Figure 5B, lower panel). Treatment with CND resulted in an enrichment of 14 canonical pathways: 3 predicted to be deactivated and 11 predicted to be activated. Only three activated pathways were shared between untreated and treated B6-D/+ males (Supplementary Table S3). Eight pathways uniquely activated in treated adults are involved in T-helper 1 cell-mediated immune responses, 5 of which involve Regulatory T cells (Tregs) (Dendritic Cell Maturation, Calcium-induced T Lymphocyte Apoptosis, ICOS-ICOSL Signaling in T Helper Cells, PKC θ Signaling in T Lymphocytes, T Cell Receptor Signaling).

Altered canonical pathways shared between untreated juvenile and adult mice

Figure 5C shows a bubble chart of the 30 canonical pathways shared between untreated B6-D/D juveniles and B6-D/+ adults. Of the 30 shared enriched pathways, 2 are predicted to be deactivated (PPAR and RHOGDI Signaling) and 28 are predicted to be activated (Figure 5D and Supplementary Table S3). The top enriched pathways (i.e., $-\log(P\text{-value}) \geq 7.0$) that are shared between juvenile and adults include Pulmonary Fibrosis Idiopathic Signaling, Osteoarthritis Pathway, Hepatic Fibrosis Signaling, S100 Family Signaling, Wound Healing Signaling, Role of JAK family kinases in IL-6-type Cytokine Signaling, and IL-6 Signaling.

Of the pathways uniquely altered in untreated juveniles, 8 were predicted to be deactivated and 11 were predicted to be activated (Figure 5D). Of those uniquely altered in untreated adults, 3 are predicted to be deactivated and 43 predicted to be activated (Figure 5D). None of the abovementioned pathways was found to be activated in juveniles or adult males treated with CND (Supplementary Table S3).

Predicted upstream regulator molecules

To identify potential drivers of the differential expression pattern observed within each dataset we used the upstream regulator function in IPA. Lipopolysaccharide (LPS), TNF, IL1B, and transforming growth factor- β (TGF- β) were the top predicted upstream activators in both untreated juveniles and adult males (including their rank order), with activation z -score ranging from 7.1 to 9.6 and 6.8 to 8.6, respectively (Supplementary Table S4). None of the z -scores was statistically significant for these upstream activators in either juvenile or adults treated with CND (Supplementary Table S4). Similarly, neither of the top predicted upstream inhibitors (also shared between) untreated juvenile and adults – APOE (z -scores: -4.0 and -4.6, respectively) and PPARGC1A (z -scores: -2.4 and -3.8, respectively) – reached statistical significance in treated juveniles and adults (Supplementary Table S4). While not appearing on the list of upstream regulators in juveniles, the top predicted upstream inhibitor for treated adults (PTGS2 or cyclooxygenase-2, z -score = -2.8) was oppositely predicted to be an upstream activator in the case of untreated adults (z -score = 2.5).

Beneficial and detrimental pathway effects

Literature searches querying cellular processes associated with canonical pathways in Supplementary Table S3 resulted in many that are commonly reported in brain injury or neurological disorders. A total of 12 such *effects* was compiled with tallies of the number of times each *effect* was involved for all 109 pathways. Many of these pathway effects are considered hallmarks of neurological disease or known to play prominent roles in disease pathogenesis or response to brain insults [38,39]. The most common pathway *effect* was ‘Neuroinflammation’ (INF), which was involved in 80 of the 109 (73.4%) pathways. This was followed by BBB (51.4%), ‘neurogenesis/repair’ (NER, 51.4%), ‘apoptosis/clearance’ (APO, 48.6%), OXS (36.7%), ‘glial activation’ (GLA, 35.8%), ‘synaptic plasticity’ (SYN, 29.4%), ‘angiogenesis’ (ANG, 27.5%), ‘secondary injury’ (SIC, 23.9%), ‘extracellular matrix’ (ECM, 17.4%), ‘neurodegeneration’ (NDG, 15.6%), and ‘fibrosis/scar formation’ (FBS, 13.8%). Juvenile versus adult effect frequencies differed slightly, with some higher in adults: APO (36.5% vs 55.7%), BBB (50.0% vs 64.6%), SIC (19.2% vs 30.4%), SYN (23.1% vs 29.1%), GLA (34.6% vs 48.1%), respectively, and OXS higher in juveniles (46.2% vs 35.4%), respectively (Figure 6A). The pathway effects most often inferred to be beneficial are ANG (86.7%), NER (85.7%), SYN (78.1%), and APO (67.9%), while the effects most often inferred to be detrimental are NDG (94.1%), FBS (93.3%), SIC (73.1%), GLA (66.7%), and BBB (64.3%).

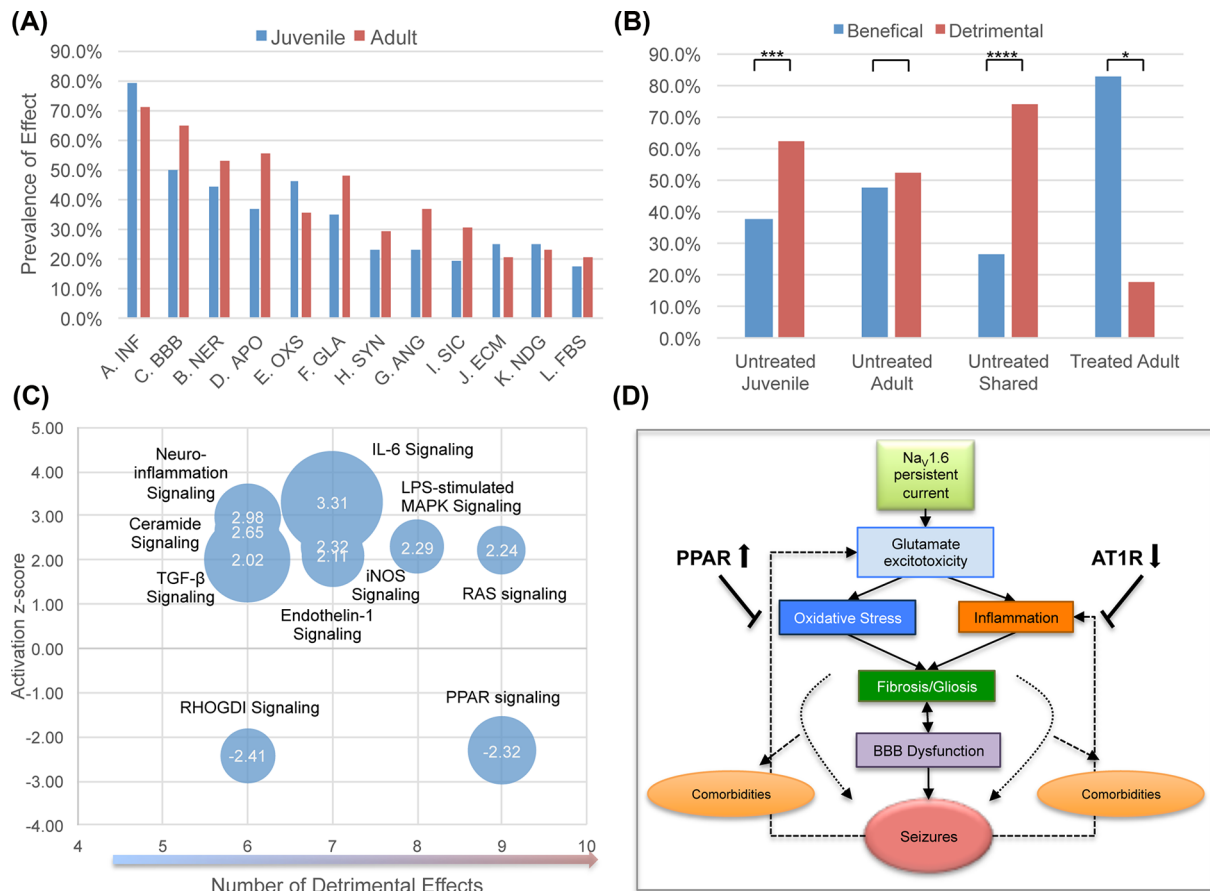


Figure 6. Detrimental and beneficial pathway effects in untreated and treated B6-D/D juvenile and B6-D/+ adult male mice (A) Bar chart showing 12 common pathway effects representing a range of injury processes associated with 109 canonical pathways identified in B6-D/D juvenile (blue) and B6-D/+ adult males (red) (Figure 5D). ANG, angiogenesis; APO, Apoptosis/clearance; BBB, blood–brain barrier; ECM, extracellular matrix; FBS, fibrosis/scar formation; GLA, glial activation; INF, neuroinflammation; NDG, neurodegeneration; NER, neurogenesis/repair; OXS, oxidative stress; SIC, secondary injury cascade; SYN, synaptic plasticity. (B) Mean frequency of beneficial and detrimental effects associated with pathways in untreated juveniles, untreated adult males, treated adults and those shared between B6-D/D juveniles and B6-D/+ adult males. (C) Top 10 most detrimental pathways among all 109 in Figure 5D plotted according to activation z-score (y-axis), number of detrimental effects (x-axis) and enrichment *P*-value (diameter of circle). (D) Integrative model for epileptogenesis indicating feedback loops potentially acted upon by CND.

The mean number of effects associated with a pathway is 4.2 ± 2.0 . Comparing the total number of detrimental and beneficial effects associated with untreated juvenile and adult pathways, we find that juveniles have a slightly higher ratio of detrimental to beneficial effects (62.3%) compared with adults (52.2%) (Figure 6B). The mean number of detrimental effects for juvenile pathways (2.6 ± 2.6) is statistically significantly higher than beneficial effects (1.6 ± 1.7) (*t*-test, *P*-value = 9.4×10^{-4}), which is not the case for adult pathways (2.5 ± 2.7 vs 2.3 ± 1.3 , respectively; *t*-test, *P*-value = 0.293). Interestingly, there is a statistically significant shift toward increased detrimental effects (73.8%) among the 33 pathways shared between untreated juvenile and adults (Figure 6B): the mean number of detrimental and beneficial effects is 3.7 ± 2.6 and 1.3 ± 1.8 , respectively (*t*-test, *P*-value = 3.4×10^{-6}). This shift toward detrimental effects is clearest for OXS (+41.7%), APO (+39.4%), NER (+32.4%), and SIC (+26.9%), with only ANG (13.3%) shifting toward beneficial. On the contrary, we find that the mean number of beneficial effects is statistically significantly greater (1.7 ± 1.7) than that for detrimental effects (0.4 ± 0.9) (*t*-test, *P*-value = 0.014) for pathways identified in treated mice (Figure 6C). Detrimental tallies were cut by more than half for nearly all of the effects (Figure 6D) other than for INF and NER. In addition, a new pathway effect appeared in treated adults: Activation of T cells (Tregs).

When we tally the number of detrimental and beneficial effects for each pathway with ≥ 3 effects, we find that 26 are inferred to be associated solely with detrimental effects and 36 solely with beneficial effects (Supplementary Table S3). The RAS and PPAR Signaling pathways are associated with the largest number of detrimental effects, each with 9 detrimental and 0 beneficial effects (Figure 6C), while the PI3K/AKT, HGF and Prolactin Signaling pathways are associated with the largest number of beneficial effects, each with 0 detrimental and 7 beneficial effects (Supplementary Table S3).

Discussion

This is the first study to test CND administration in a mouse model with a natural onset of seizures, and to investigate the cellular and molecular mechanisms involved in improved outcomes. The results indicate significant efficacy of CND from three perspectives: survival and seizure frequency, BBB function, and genome-wide hippocampal gene expression. The findings of extended lifespan, longer seizure-free periods, and reduced seizure frequency in Scn8a-N1768D mice treated with CND are robust to age, sex, and strain background (Figures 2 and 3). We previously tested cannabidiol (CBD) on B6-D/+ and B6-D/D mice and found that males (but not females) benefited with increased survival and reduced seizure frequencies: B6-D/+ adult and B6-D/D juvenile males survived for a mean of 17.4 (18.2%, *t*-test, *P*-value = 4.5×10^{-3}) 2.5 (10.2%, *t*-test, *P*-value = 0.032) days longer, while each experienced reduced seizure frequencies of 31.3% and 44.0%, respectively [20]. Treatment with CND yielded greater increases in survival, with B6-D/+ males surviving for a mean of 44.5 days longer (48.9%, *t*-test *p*-value = $<1.0 \times 10^{-5}$) and B6-D/D males surviving for 6.3 days longer (27%, *t*-test, *P*-value = $<1.0 \times 10^{-5}$). These increases represent larger standard effect sizes of 0.69 and 0.79, respectively, compared with 0.50 and 0.35 for CBD-treated B6-D/+ and B6-D/D males [20]. In addition, CND treatment resulted in greater reductions in seizure frequency for B6-D/+ males (56.5%) and B6-D/D juveniles (45.8%). The present study found CND also outperformed phenytoin – an anti-seizure medication shown to be efficacious for patients with SCN8A [40], in terms of survival in juvenile Scn8a-D/D mice. While phenytoin showed a greater reduction in post-onset seizure frequency, CND provided significant improvements in both survival and seizure control. The same mouse model was used to test chronic administration with Prax-330 (GS967) – a novel sodium channel modulator [41]. While we couldn't make direct comparisons with testing on B6-D/+ adults due to differences in study design, Prax-330 treatment of B6-D/D mice yielded an increased survival of 5.7 days (29.8%), representing a slightly smaller standard effect size (0.69) as we found for CND.

We also found that adult B6-D/+ females and males both exhibit significantly reduced BBB 'leak' when treated with CND after the establishment of seizures (Figure 4). Untreated B6-D/D juvenile and B6-D/+ adult males exhibited significant 'disease-induced' genome-wide changes in hippocampal transcript abundance, many of which were returned to physiological levels in treated mice. Characterization of enriched pathways in untreated mice revealed a host of cellular and molecular processes representing both adaptive and maladaptive responses to increased neuronal excitability (Supplementary Table S3).

In the following sections we discuss physiological effects of Scn8a-induced neuronal hyperexcitability in the context of the juvenile and adult brain, and then ask whether the known mechanism(s) of action of ARBs can explain our findings of improved outcomes in CND-treated mice. We used a 'two-prong approach' to determining how administration of CND impacts the injury cascade following seizure onset in this model. First, we compare disease-induced pathway alterations in untreated mice with those that are expected to occur after increased AT1R signaling in various disease models. Then we turn to the drug-induced pathway alterations and ask whether they are consistent with the known mechanism of action (MoA) of CND. ARBs are known to have a dual MoA resulting from AT1R antagonism and partial PPAR γ agonism. Our comparative analysis evaluates whether observed pathway alterations reflect predicted effects of these MoAs in untreated and treated mice.

Hippocampal gene expression signatures of untreated juvenile and adult mice

At baseline, the excitability of the juvenile or neonatal brain differs from that of the adult brain. In neonates and juveniles, the brain is undergoing rapid growth and maturation, with ongoing synaptogenesis, dendritic arborization, and myelination. These developmental processes affect the balance between excitation and inhibition, making the immature brain more prone to hyperexcitability compared with the fully matured adult brain [42–44]. The more detrimental pattern in juveniles (Figure 6B) along with the increased number of DEGs (Figure 5B), may indicate increased vulnerability to the harmful effects of seizures. Despite these differences there are many similarities in the ways juvenile and adult brains respond to epileptic conditions. In this section we compare genome-wide patterns of transcript abundance in untreated juveniles and adult males, first on shared pathways and then on unique aspects

of each age group. For a more complete discussion of genome-wide changes in gene expression in untreated adult B6-D/+ females and males, see [6].

Shared pathways

Figure 5C shows the 32 pathways shared by untreated juvenile and adults.

Identification in independent experiments lends credence to the veracity of the enrichment results and the importance of these pathways in the epileptic brain. The topmost significantly activated pathways (mean $-\log(P\text{-values}) \geq 7.0$) include pulmonary fibrosis idiopathic signaling, S100 family signaling, wound healing, hepatic fibrosis signaling, role of JAK family kinases in IL-6 type cytokine signaling, IL-6 signaling, and osteoarthritis signaling (Figure 5). In the context of the CNS, activation of the two fibrosis pathways implicates the process of astrogliosis and processes involving TGF- β signaling (also activated in both age groups), extracellular matrix (ECM) remodeling, and collagen deposition [45]. In addition to TGF- β , these pathways share a subset of genes with wound healing, including collagens and laminins that comprise the basement membrane component of the BBB [6]. While initially beneficial, these processes can be exacerbated after seizures are established, leading to BBB dysfunction, astrogliosis and scar formation [45]. Indeed, direct activation of the TGF- β pathway by TGF- β 1 – one of the top predicted activators in untreated mice – results in epileptiform activity similar to that after exposure to albumin [46]. S100 family signaling proteins are known to function in stress responses and a variety of Ca^{2+} -dependent intracellular functions and represent biomarkers of neuronal injury [47,48]. The JAK-STAT signaling pathway, including the JAK family of kinases and IL-6 cytokine signaling are known to play a significant role in neuroinflammation following brain injury [49], including in the development of epilepsy [50].

Deactivation of RHODGI and PPAR signaling (discussed below) were also found for both age groups (Figure 5C). The deactivation of RHODGI, a negative regulator of the Rho family of GTPases, can result in the constitutive activation of multiple Rho GTPases, including RhoA2 and its downstream effector Rho kinase (ROCK) [51–53]. This in turn can promote actin cytoskeleton rearrangements in brain microvascular endothelial cells, leading to increased permeability of the BBB [54,55]. Activating the RhoA/ROCK1 pathways also has been linked to neuronal death and subsequent production of tumor necrosis factor- α (TNF- α) and IL-1 β after traumatic brain injury (TBI) [56].

We note a clear enhancement in detrimental effects associated with shared pathways (Figure 6B). Pathways with the most detrimental effects ($n \geq 6$) include both deactivated pathways (PPAR and RHODGI signaling), and the six activated pathways with asterisks in Figure 5C: LPS-stimulated MAPK signaling, IL-6 Signaling, iNOS signaling, Neuroinflammation Signaling, TGF- β signaling, and role of JAK family kinases in IL-6-type cytokine signaling. The detrimental nature of the effects of these activated pathways may represent the signal of an advanced neuroinflammatory process, possibly mediated by activated M1 pro-inflammatory microglia [57]. The pro-inflammatory cytokines produced through the LPS-stimulated MAPK and HMGB1 signaling pathways can lead to a cytokine storming [58] and the propagation of seizure activity [59,60]. Despite this increased detrimental signal among shared pathways, we note activation of some pathways with potential beneficial effects, such as RAC, Paxillin and FAK signaling – which may represent compensatory mechanisms to protect against BBB dysfunction and mitigate inflammatory responses during chronic injury [61–63] (Figure 6C).

Pathways unique to juveniles

There were 19 dysregulated pathways unique to juveniles (Figure 5D; Supplementary Table S3). Activation of CSDE1 signaling could potentially influence multiple pathways as it results in increases and decreases in the abundance of RNAs [64]. Activation of the production of nitric oxide and reactive oxygen species (ROS) by activated macrophages contributes to OXS and neuroinflammation, which can further exacerbate neuronal damage [57,65,66]. This inflammatory milieu may also activate signaling pathways such as TNFR1 and TNFR2 signaling, which mediate the effects of TNF- α on immune responses and cell survival [67]. The deactivation of eicosanoid signaling may result in prolonged inflammation and impaired resolution of neuroinflammation, exacerbating neuronal damage and tissue injury [68,69]. Additionally, OXS potentially can impact pathways such as white adipose tissue browning and urate biosynthesis/inosine 5'-phosphate degradation, which are sensitive to cellular redox status and metabolic changes [70].

Eleven of the 19 altered juvenile pathways are involved in cellular metabolism, energy homeostasis and neurotransmitter metabolism (Supplementary Table S3). While there isn't a single common pathway that regulates all these pathways, metabolic pathways involved in nucleotide degradation (adenosine, purine, and guanosine), urea biosynthesis, and ethanol degradation are interconnected and regulated by common metabolic enzymes and signaling pathways.

For example, the enzymes involved in the degradation pathways of ethanol, leucine, histamine, noradrenaline, and dopamine (many of which localized in mitochondria) may be sensitive to OXS [8,71]. In response to seizures,

the antioxidant defense mechanisms may be activated to counteract oxidative damage and potentially modulate the activity of these enzymes [72,73].

Effects of CND treatment on gene expression signatures in juvenile and adult mice

The greatly reduced number of DEGs, and the lack of significant pathway enrichment in juveniles treated with CND (Figure 5B) reflects transcript abundance patterns similar to those under physiological conditions. In treated juveniles, a relaxed FDR revealed a significant enrichment signal for OXPHOS and EIF2 signaling pathways. This pattern is very similar to that observed in untreated pre-seizure females, which was discussed previously [6]. Briefly, we suggested that the increase in OXPHOS gene expression was a beneficial response to cellular stress and the depletion of ATP in the hyperexcitable state before seizure onset [74,75]. The coordinated activation of EIF2 signaling may have represented a compensatory mechanism providing for the production of proteins involved in the ETC [76–78]. CND treatment may induce a similar process, boosting mitochondrial function in a manner similar to the mitohormesis effect observed in exercise-trained mice [75,79]. In so doing, CND treatment may have shifted the metabolic and redox balance toward physiological conditions.

Similar to juveniles, treated adults exhibited genome-wide transcript abundance profiles approximating those under physiological conditions; however, there was a set of 8 canonical pathways exclusively activated in treated adult males (Supplementary Table S3), 5 of which are involved in modulating the immune response [80–82] – specifically in enhancing the activation of Tregs. Tregs are a subset of T cells that play a crucial role in immune tolerance (i.e., dampening excessive immune responses and promoting immune homeostasis) [82,83]. Tregs have been shown to protect against pathological neuroinflammation by polarizing microglia toward a M2-like phenotype [84] in several injury models [84–86]. In epilepsy, brain Treg depletion reduces neuronal survival and exacerbates hippocampal neuroinflammation and OXS and after SE, while Treg enhancement exerts an antiepileptic effect [87]. The anti-inflammatory milieu so produced may protect neurons from secondary damage and contribute to the maintenance of seizure control by reducing excitability of neuronal networks and minimizing risk of seizure recurrence [87]. It is not possible to infer whether treatment with CND directly or indirectly led to the activation of Tregs and the long-term stabilization of the immune response.

Another interesting finding is the activation of the macrophage alternative activation signaling pathway (Supplementary Table S3). This pathway (also known as the ‘M2’ macrophage activation pathway), plays a significant role in the resolution of inflammation, tissue repair, and remodeling. In the early phases of CNS injury, skewing of microglia and macrophages toward pro-inflammatory M1-like phenotype is adaptive (e.g., aids in clearing dead cells and debris). Over time, switching to a M2-like anti-inflammatory phenotype promotes improved tissue repair and remodeling, BBB integrity, angiogenesis, and neuronal survival [65,88].

Are the effects of Scn8a-induced gene expression patterns consistent with the pathological effects of RAS as mediated by AT1Rs?

Many of the pathological conditions that are known to occur during epileptogenesis also occur in the Scn8a-N1768D mouse (Supplementary Table S3). Figure 6D presents an interactive model in which neuronal hyperexcitability associated with persistent $\text{Na}_v 1.6$ current triggers a sequential chain including glutamate excitotoxicity, calcium overload, OXS/MD, inflammatory responses, glial activation, BBB dysfunction, fibrosis, and seizures. The model includes several feedback loops and highlights the importance of neuroinflammatory processes [89].

Likewise, in the context of various brain disorders and injuries, Ang II is increased and AT1R signaling activated, triggering release of pro-inflammatory cytokines via activation of NF- κ B expression and leading to an injury cascade characterized by many of the abovementioned pathological processes [10,11,90–93]. Indeed, increased Ang II has been shown to play a pathophysiological role in epilepsy [16,17,94–97]. Experiments with LPS, which also activates AT1R signaling, point to positive feedback between Ang II and inflammation [98]. Additionally, there is crosstalk between the RAS and PPAR signaling pathways as AT1R overstimulation inhibits PPAR γ [92] (see below).

Activation of AT1Rs involves stimulating kinase pathways, such as mitogen-activated protein kinases (MAPK, p38) and JAK/STAT pathways [11]. MAPK signaling was inferred to be activated in both untreated juvenile and adult mice as evidenced by activation of LPS-stimulated MAPK signaling and p38 MAPK signaling (Supplementary Table S3). Neuroinflammation can also be mediated by the release of damage associated molecular pattern mediators (DAMPs), which trigger inflammatory responses from microglia, astrocytes, and neurons [11,89]. Indeed, HMGB1 signaling was inferred to be activated in both untreated juvenile and adult mice, as were IL-6 signaling, neuroinflammation

signaling, pathogen induced cytokine storm signaling, and JAK family kinases in IL-6-type cytokine storm signaling pathways (Supplementary Table S3).

Our results reveal that activation of the renin–angiotensin signaling and deactivation of PPAR signaling pathway are associated with the largest number of detrimental effects of any pathway in Supplementary Table S3 (Figure 6C). The top predicted upstream activators for both juveniles and adult males (LPS, TNF- α , IL-1B, and TGFB1) are key mediators of inflammation and inducible by Ang II via microglia activation [92,99] (Supplementary Table S4). The top predicted upstream inhibitor was PPARGC1A (PGC-1 α), a coactivator recruited during PPAR stimulation. Among the targets of PGC-1 α are several mitochondria-related genes that play important roles in mitochondrial oxidative metabolism and biogenesis, as well as in the maintenance of intracellular calcium levels [100]. We infer from these results that Scn8a pathophysiology closely mimics (and may indirectly result from or converge on) the pathological processes associated with overstimulation of AT1R and deactivation of PPAR signaling.

Are the effects of CND treatment consistent with the known mechanism of action of ARBs?

Nearly all of the above pathway alterations identified in untreated were ‘normalized’ (i.e., no longer significantly enriched by DEGs) in both treated juvenile and adult male mice (Supplementary Table S3). Here we evaluate whether the known MOAs of CND can explain these results. ARBs are known to have powerful anti-inflammatory, anti-fibrotic, and antioxidant activities [11,13,14]. The anti-inflammatory action of ARBs may involve both their AT1R antagonist and partial PPAR γ agonist activities. One of the known anti-inflammatory effects of ARBs derives from their ability to inhibit HMGB1 signaling (see above) [11]. Activation of widely expressed PPAR receptors leads to additional anti-inflammatory, neuroprotective, and metabolic effects [14]. PPAR γ agonism can block NF- κ B signaling in the brain, reduce the production of ROS, mitigate microgliosis, and promote mitochondrial function [14,101]. It is important to note that AT1R blockade and PPAR γ agonism can act as independent anti-inflammatory mechanisms; however, as stated above, AT1R signaling suppresses PPAR γ induction and PPAR γ signaling reduces AT1R activation [11].

In animal models of TBI, AT1R blockade has been shown to reduce OXS and stabilize the BBB. CND in particular has consistently demonstrated beneficial effects by reducing expression of genes involved in the inflammatory response and microglia activation, and by inhibiting IL-6, IL-1 β , iNOS, TNF- α , and TGF- β 1 signaling. By inhibiting signaling of the pro-fibrotic cytokine TGF β , ARBs can modulate ECM remodeling, reduce fibrosis and gliotic scar formation, and mitigate the development of recurrent seizures [11]. Most of the studies that have explored the use of ARBs to control vulnerability to seizures [16] have focused on losartan. This ARB was shown to mitigate BBB breakdown and status epilepticus (SE)-induced epileptogenesis in rats by blocking TGF β signaling [15,102], and to inhibit production of ROS by preventing NOX2 activation [15,17,103–105]. BBB dysfunction and gliosis were improved in a rat pilocarpine model [103]. Treatment with another ARB, telmisartan, reduced seizure frequency in dogs [106].

We were not able to find another published study that examined the effects of CND directly in an epilepsy model; however, a number of studies have examined CND effects in related models. For example, CND was able to suppress acute hypoxia-induced seizures and reduce later-life seizure susceptibility in a neonatal mouse hypoxia model [107]. In rats treated with LPS, CND administration ameliorated microglial activation, reduced NF- κ B signaling, and lowered the level of COX-2 and the generation of ROS [108,109]. Treatment of neuronal cells with CND normalized the expression of hundreds of genes associated with glutamate-induced inflammation, diabetes signaling, and amyloid β metabolism [9]. Similar to this study, the top predicted upstream activators for neuronal cells stimulated with excitotoxic levels of glutamate (and down-regulated by CND) included LPS, TNF- α , IL-1B, and TGFB1 (Supplementary Table S4).

While we cannot tease apart the relative roles of AT1R and PPAR signaling in adults, PPAR agonism may play a larger role in the juvenile case. RAS signaling is not activated in untreated juveniles, and there is indirect evidence for increased detrimental effects of OXS (Figure 6A). The beneficial effects of CND treatment may thus relate to its ability to induce PPAR γ activity, which is known to mitigate OXS and tissue damage. Indeed, the PPAR γ agonist pioglitazone has been shown to increase the expression of ETC subunit proteins [101]. In the case of the adult brain, CND treatment produced an ‘anti-similar’ result in which cyclooxygenase-2 (COX-2) was predicted as an upstream activator in untreated adults and as an upstream inhibitor in treated mice (Supplementary Table S4). Both AT1R blockade and PPAR activation mediate down-regulation of a wide array of pro-inflammatory mediators in microglia, including TNF- α , IL-1 β , IL-6, iNOS, and COX-2 [13,14] (Supplementary Figure S5). Under pathologic conditions, COX-2 activity can produce ROS and toxic prostaglandin metabolites that can exacerbate brain injury [110]. A similar anti-similar pattern held for ERBB2 and NUPR1, the latter is activated in response to OXS [111]. Inhibition of ErbB

receptor activity, which is elevated in reactive astrogliosis, suppresses hypertrophic remodeling via reduced Src/FAK activity [112].

Conclusions and challenges

These results support the hypothesis that the efficacy of CND in our novel model of epileptogenesis is related to its known dual MoA [11] (Figure 6 D). The robust efficacy of CND across ages, sexes and mouse strains is a positive indication for successful translation and drug repurposing in humans. Evidence for its efficacy in the context of the juvenile brain is critical given the early onset of seizures in children with SCN8A-related epilepsy. Interestingly, results of recent large cohort studies of adults with hypertension indicated that use of ARBs was associated with a significantly decreased incidence of epilepsy compared with other classes of antihypertensive drugs [113,114]. Importantly, the use of CND has been approved to treat hypertension in adolescents and children aged one and older, reflecting its excellent safety profile and suitability for use in clinical trials for children with SCN8A epilepsy [115]. In terms of lifetime survival in Scn8a-D/D juveniles, CND outperformed PHT – an often-prescribed ASM for epilepsy [40]. In contrast with many ASMs that primarily target ion channels or neurotransmitter systems to reduce seizure occurrence, ARBs appear to address underlying pathological processes involved in epileptogenesis, such as inflammation, oxidative stress, and BBB dysfunction. Importantly, the effect of CND on gene expression and multiple pathological processes suggest it may offer broader neuroprotective benefits beyond seizure control. Interestingly, removal of administration of Prax-330 from B6-D/+ mice resulted in rapid loss of protection, suggesting that it acts primarily as an anticonvulsant rather than a disease-modifying therapy [41]. Future studies of CND and gene-based treatments [116] will help to assess to what extent these different therapeutic approaches are truly disease-modifying. Alternatively, treatment strategies incorporating CND as an adjuvant with sodium channel blockers may also yield improved outcomes for seizures and co-morbid conditions [16]. Finally, many cellular and molecular processes identified here are shared with other forms of epilepsy [6], brain injury [117], and inflammatory brain disorders [6,10,12,39]. In that light, the translational data set presented in this study supports the hypothesis that ARBs may be a useful therapeutic strategy for other neurodevelopmental disorders with similar primary hallmarks [12,39].

Challenges

The response to brain insult is highly complex, involving a multitude of signaling pathways that interact in a dynamic and context-dependent manner. The balance between these signals can influence whether the outcome leans more towards regeneration and recovery or towards scar formation and chronic impairment [118]. Many pathways represent a *double-edged sword* in that they are associated with both beneficial and detrimental effects, depending on the temporality, duration, and magnitude of pathway (de)activation, as well as on the specific cellular and molecular context in which the pathway(s) operate [66,119,120]. In general, we interpreted the effects of pathway alterations under the assumption that they were occurring in the later stages of epileptogenesis (i.e., after the establishment of spontaneous recurrent seizures). One advantage of the systems approach taken here is that comparison of drug-induced gene expression profiles can identify potential off-targets [32] – of which few, if any, were identified. We also faced the previously discussed methodological challenge [6] of false positives called by IPA [121]. The approach taken here helped to mitigate this issue to some extent by focusing on a set of the most informative and commonly reported pathway effects (Supplementary Table S3). This form of ‘feature selection’ reduces the impact of false positives. None of the 12 pathway effects were highly correlated suggesting that this set of effects captures distinct features of clinical presentation. However, we note that alternative inferences regarding beneficial or detrimental effects are possible and that additional features/effects may have been excluded.

Clinical perspectives

- Epilepsy is a common neurological disease; however, few if any of the currently marketed antiseizure medications prevent or cure epilepsy. Angiotensin receptor blockers (ARBs) represent a promising strategy to treat the numerous detrimental consequences of epileptogenesis.
- Scn8a pathology mimics the known effects of angiotensin type 1 receptor (AT1R) overstimulation and thus, blocking AT1R activation has potential therapeutic value in this model and other neurological disorders with similar pathological features.

- Results of testing candesartan, an FDA-approved ARB indicated for hypertension in pediatric patients older than 1 year, on this transgenic Scn8a mouse model yield strong evidence for its efficacy and support its use in clinical trials for children with SCN8A-related epilepsy.

Data Availability

The data that support the findings of the present study are available from the corresponding author on reasonable request. Raw data of RNA sequencing have been submitted to the Figshare repository at https://portlandpress.figshare.com/articles/dataset/RNAseq_readcount_files_for_untreated_and_treated_juveniles/26417218

Competing Interests

The authors declare that there are no competing interests associated with the manuscript.

Funding

P.T.R. was funded by a Translational Research Grant from the American Heart Association [grant number 19TPA34910113]. This work was also supported by funding from the Shay Emma Hammer Research Foundation.

Open Access

Open access for this article was enabled by the participation of University of Arizona in an all-inclusive *Read & Publish* agreement with Portland Press and the Biochemical Society under a transformative agreement with Individual.

CRedit Author Contribution

Michael F. Hammer: Conceptualization, Resources, Data curation, Formal analysis, Supervision, Funding acquisition, Validation, Investigation, Visualization, Methodology, Writing—original draft, Project administration, Writing—review & editing. **Erfan Bahramnejad:** Data curation, Investigation, Methodology. **Joseph C. Watkins:** Formal analysis, Validation. **Patrick T. Ronaldson:** Data curation, Formal analysis, Funding acquisition, Writing—original draft.

Ethics Statement

Ethical approval for animal work was obtained from the University of Arizona Institutional Animal Care and Use Committee Program (IACUC #16-160). All experiments were designed in accordance with the Animal Research: Reporting In Vivo Experiments (ARRIVE) guidelines. Animal experiments were conducted in approved facilities in the laboratories of MH and PTR at the University of Arizona. At the conclusion of each experiment or when necessary due to morbidity, animals were euthanized using ketamine/xylazine followed by cervical dislocation.

We confirm that we have read the Journal's position on issues involved in ethical publication and affirm that this report is consistent with those guidelines.

Acknowledgements

We thank Aurora Hurtado, Emily Barnes, Joshua Hack and Sarah Lester for technical support. We also thank the Shay Emma Hammer Research Foundation for funding.

Abbreviations

ANG, angiogenesis; AngII, Angiotensin II; APO, apoptosis/clearance; ARB, angiotensin receptor blocker; ARRIVE, Animal Research: Reporting In Vivo Experiments; ASM, antiseizure medication; AT1R, angiotensin type 1 receptor; ATP, adenosine triphosphate; B6, C57BL/6J; BBB, blood–brain barrier; BBBD, blood–brain barrier dysfunction; C3H, C3H/HeJ; CND, candesartan; COX-2, cyclooxygenase-2; CSDE1, Cold Shock Domain Containing E1; DAMP, damage-associated molecular pattern mediator; DEG, differentially expressed genes; ECM, extracellular matrix; EIF2, eukaryotic initiation factor 2; ERBB2, erythroblastic oncogene B; ETC, electron transport chain; FAK, focal adhesion kinase; FBS, fibrosis/scar formation; FDA, Food and Drug Administration; FDR, false discovery rate; GLA, glial activation; HGF, hepatocyte growth factor; HMGB1, high-mobility group box 1; IACUC, Institutional Animal Care and Use Committee Program; INF, neuroinflammation; iNOS, inducible nitric oxide synthase; IPA, Ingenuity[®] Pathway Analysis; LPS, lipopolysaccharide; MAPK, mitogen-activated protein kinases; MD, mitochondrial dysfunction; MDS, multidimensional scaling; MoA, mechanism of action; NDG, neurodegeneration; NER, neurogenesis/repair; Nox2, NADPH oxidase 2; NUPR1, nuclear protein 1; OXPHOS, oxidative phosphorylation; OXS, oxidative stress; PGC-1 α , peroxisome proliferator-activated receptor- γ coactivator; PHT, phenytoin; PI3K/Akt, phosphoinositide-3-kinase/protein kinase B;

PPAR, peroxisome proliferator-activated receptor; RAS, renin–angiotensin system; RHODGI, Rho GDP-dissociation inhibitor; ROCK, Rho-associated coiled-coil containing protein kinase; ROS, reactive oxygen species; s.c., subcutaneous; SIC, secondary injury cascade; Src, proto-oncogene tyrosine-protein kinase; STAT, Janus kinase; SYN, synaptic plasticity; TBI, traumatic brain injury; TC, tonic-clonic seizure; TGF- β , transforming growth factor- β ; TNF- α , tumor necrosis factor- α ; TNFR, tumor necrosis factor receptor; Tregs, regulatory T cells; VEH, vehicle.

References

- Sands, T.T. and Gelinias, J.N. (2024) Epilepsy and encephalopathy. *Pediatr. Neurol.* **150**, 24–31, <https://doi.org/10.1016/j.pediatrneurol.2023.09.019>
- Nevin, S.M., Wakefield, C.E., Schilstra, C.E., McGill, B.C., Bye, A. and Palmer, E.E. (2020) The information needs of parents of children with early-onset epilepsy: A systematic review. *Epilepsy Behav.* **112**, 107382, <https://doi.org/10.1016/j.yebeh.2020.107382>
- Hammer, M.F., Xia, M. and Schreiber, J.M. (2023) *SCN8A-Related Epilepsy and/or Neurodevelopmental Disorders* (Adam, M.P., Mirzaa, G.M., Pagon, R.A., Wallace, S.E., Bean, L.J.H., Gripp, K.W. et al., eds), GeneReviews(R), Seattle (WA)
- Zybura, A., Hudmon, A. and Cummins, T.R. (2021) Distinctive properties and powerful neuromodulation of Na(v)1.6 sodium channels regulates neuronal excitability. *Cells* **10**, 1595–1618, <https://doi.org/10.3390/cells10071595>
- Chung, K.M., Hack, J., Andrews, J., Galindo-Kelly, M., Schreiber, J., Watkins, J. et al. (2023) Clinical severity is correlated with age at seizure onset and biophysical properties of recurrent gain of function variants associated with SCN8A-related epilepsy. *Epilepsia* **64** (12), 3365–3376, <https://doi.org/10.1111/epi.17747>
- Hammer, M.F., Krzyzaniak, C.T., Bahramnejad, E., Smelser, K.J., Hack, J.B., Watkins, J.C. et al. (2024) Sex differences in physiological response to increased neuronal excitability in a knockin mouse model of pediatric epilepsy. *Clin. Sci. (Lond.)* **138**, 205–223, <https://doi.org/10.1042/CS20231572>
- Maguire, J. (2016) Epileptogenesis: more than just the latent period. *Epilepsy Curr.* **16**, 31–33, <https://doi.org/10.5698/1535-7597-16.1.31>
- Lukawski, K. and Czuczwar, S.J. (2023) Oxidative stress and neurodegeneration in animal models of seizures and epilepsy. *Antioxidants (Basel)* **12**, 1049–1078, <https://doi.org/10.3390/antiox12051049>
- Elkahloun, A.G., Hafko, R. and Saavedra, J.M. (2016) An integrative genome-wide transcriptome reveals that candesartan is neuroprotective and a candidate therapeutic for Alzheimer's disease. *Alzheimers Res. Ther.* **8**, 5, <https://doi.org/10.1186/s13195-015-0167-5>
- Saavedra, J.M. (2012) Angiotensin II AT(1) receptor blockers as treatments for inflammatory brain disorders. *Clin. Sci. (Lond.)* **123**, 567–590, <https://doi.org/10.1042/CS20120078>
- Villapol, S., Janatpour, Z.C., Afram, K.O. and Symes, A.J. (2023) The renin angiotensin system as a therapeutic target in traumatic brain injury. *Neurotherapeutics* **20**, 1565–1591, <https://doi.org/10.1007/s13311-023-01435-8>
- Saavedra, J.M. (2017) Beneficial effects of Angiotensin II receptor blockers in brain disorders. *Pharmacol. Res.* **125**, 91–103, <https://doi.org/10.1016/j.phrs.2017.06.017>
- Benicky, J., Sanchez-Lemus, E., Honda, M., Pang, T., Orecna, M., Wang, J. et al. (2011) Angiotensin II AT1 receptor blockade ameliorates brain inflammation. *Neuropsychopharmacology* **36**, 857–870, <https://doi.org/10.1038/npp.2010.225>
- Cai, W., Yang, T., Liu, H., Han, L., Zhang, K., Hu, X. et al. (2018) Peroxisome proliferator-activated receptor gamma (PPARgamma): A master gatekeeper in CNS injury and repair. *Prog. Neurobiol.* **163–164**, 27–58, <https://doi.org/10.1016/j.pneurobio.2017.10.002>
- Bar-Klein, G., Cacheaux, L.P., Kamintsky, L., Prager, O., Weissberg, I., Schoknecht, K. et al. (2014) Losartan prevents acquired epilepsy via TGF-beta signaling suppression. *Ann. Neurol.* **75**, 864–875, <https://doi.org/10.1002/ana.24147>
- Ivanova, N. and Tchekalarova, J. (2019) The Potential therapeutic capacity of inhibiting the brain renin-angiotensin system in the treatment of co-morbid conditions in epilepsy. *CNS Drugs* **33**, 1101–1112, <https://doi.org/10.1007/s40263-019-00678-4>
- Pereira, M.G., Becari, C., Oliveira, J.A., Salgado, M.C., Garcia-Cairasco, N. and Costa-Neto, C.M. (2010) Inhibition of the renin-angiotensin system prevents seizures in a rat model of epilepsy. *Clin. Sci. (Lond.)* **119**, 477–482, <https://doi.org/10.1042/CS20100053>
- Sun, H., Wu, H., Yu, X., Zhang, G., Zhang, R., Zhan, S. et al. (2015) Angiotensin II and its receptor in activated microglia enhanced neuronal loss and cognitive impairment following pilocarpine-induced status epilepticus. *Mol. Cell. Neurosci.* **65**, 58–67, <https://doi.org/10.1016/j.mcn.2015.02.014>
- Tchekalarova, J., Loyens, E. and Smolders, I. (2015) Effects of AT1 receptor antagonism on kainate-induced seizures and concomitant changes in hippocampal extracellular noradrenaline, serotonin, and dopamine levels in Wistar-Kyoto and spontaneously hypertensive rats. *Epilepsy Behav.* **46**, 66–71, <https://doi.org/10.1016/j.yebeh.2015.03.021>
- Bahramnejad, E., Barney, E.R., Lester, S., Hurtado, A., Thompson, T., Watkins, J.C. et al. (2023) Greater female than male resilience to mortality and morbidity in the Scn8a mouse model of pediatric epilepsy. *Int. J. Neurosci.* **6**, 1–13, <https://doi.org/10.1080/00207454.2023.2279497>
- Percie du Sert, N., Hurst, V., Ahluwalia, A., Alam, S., Avey, M.T., Baker, M. et al. (2020) The ARRIVE guidelines 2.0: Updated guidelines for reporting animal research. *J. Cereb. Blood Flow Metab.* **40**, 1769–1777, <https://doi.org/10.1177/0271678X20943823>
- Villapol, S., Yaszemski, A.K., Logan, T.T., Sanchez-Lemus, E., Saavedra, J.M. and Symes, A.J. (2012) Candesartan, an angiotensin II AT(1)-receptor blocker and PPAR-gamma agonist, reduces lesion volume and improves motor and memory function after traumatic brain injury in mice. *Neuropsychopharmacology* **37**, 2817–2829, <https://doi.org/10.1038/npp.2012.152>
- Yan, W.H., Pan, C.Y., Dou, J.T., Meng, J.H., Wang, B.A. and Mu, Y.M. (2016) Candesartan cilxetil prevents diet-induced insulin resistance via peroxisome proliferator-activated receptor-gamma activation in an obese rat model. *Exp Ther Med.* **12**, 272–278, <https://doi.org/10.3892/etm.2016.3297>
- Song, H., Tufa, U., Chow, J., Sivanenthiran, N., Cheng, C., Lim, S. et al. (2018) Effects of antiepileptic drugs on spontaneous recurrent seizures in a novel model of extended hippocampal kindling in mice. *Front Pharmacol.* **9**, 451, <https://doi.org/10.3389/fphar.2018.00451>
- Abdullahi, W., Tripathi, D. and Ronaldson, P.T. (2018) Blood-brain barrier dysfunction in ischemic stroke: targeting tight junctions and transporters for vascular protection. *Am. J. Physiol. Cell Physiol.* **315**, C343–C356, <https://doi.org/10.1152/ajpcell.00095.2018>

- 26 Brzica, H., Abdullahi, W., Reilly, B.G. and Ronaldson, P.T. (2018) Sex-specific differences in organic anion transporting polypeptide 1a4 (Oatp1a4) functional expression at the blood-brain barrier in Sprague-Dawley rats. *Fluids Barriers CNS* **15**, 25, <https://doi.org/10.1186/s12987-018-0110-9>
- 27 Ronaldson, P.T., Demarco, K.M., Sanchez-Covarrubias, L., Solinsky, C.M. and Davis, T.P. (2009) Transforming growth factor-beta signaling alters substrate permeability and tight junction protein expression at the blood-brain barrier during inflammatory pain. *J. Cereb. Blood Flow Metab.* **29**, 1084–1098, <https://doi.org/10.1038/jcbfm.2009.32>
- 28 Sultan, F.A. (2013) Dissection of different areas from mouse hippocampus. *Bio Protoc* **3**, <https://doi.org/10.21769/BioProtoc.955>
- 29 Dobin, A., Davis, C.A., Schlesinger, F., Drenkow, J., Zaleski, C., Jha, S. et al. (2013) STAR: ultrafast universal RNA-seq aligner. *Bioinformatics* **29**, 15–21, <https://doi.org/10.1093/bioinformatics/bts635>
- 30 Anders, S., Pyl, P.T. and Huber, W. (2015) HTSeq—a Python framework to work with high-throughput sequencing data. *Bioinformatics* **31**, 166–169, <https://doi.org/10.1093/bioinformatics/btu638>
- 31 Robinson, M.D., McCarthy, D.J. and Smyth, G.K. (2010) edgeR: a Bioconductor package for differential expression analysis of digital gene expression data. *Bioinformatics* **26**, 139–140, <https://doi.org/10.1093/bioinformatics/btp616>
- 32 Szalal, B. and Veres, D.V. (2023) Application of perturbation gene expression profiles in drug discovery—From mechanism of action to quantitative modelling. *Front Syst. Biol.* **3**, 1–11, <https://doi.org/10.3389/fsysb.2023.1126044>
- 33 Hammer, M.F., Sprissler, R., Bina, R.W., Lau, B., Johnstone, L., Walter, C.M. et al. (2019) Altered expression of signaling pathways regulating neuronal excitability in hippocampal tissue of temporal lobe epilepsy patients with low and high seizure frequency. *Epilepsy Res.* **155**, 106145, <https://doi.org/10.1016/j.eplepsyres.2019.05.013>
- 34 Sprissler, R., Bina, R., Kasoff, W., Witte, M.H., Bernas, M., Walter, C. et al. (2019) Leukocyte expression profiles reveal gene sets with prognostic value for seizure-free outcome following stereotactic laser amygdalohippocampotomy. *Sci. Rep.* **9**, 1086, <https://doi.org/10.1038/s41598-018-37763-5>
- 35 Schurch, N.J., Schofield, P., Gierlinski, M., Cole, C., Sherstnev, A., Singh, V. et al. (2016) How many biological replicates are needed in an RNA-seq experiment and which differential expression tool should you use? *RNA* **22**, 839–851, <https://doi.org/10.1261/rna.053959.115>
- 36 Lochhead, J.J., Yang, J., Ronaldson, P.T. and Davis, T.P. (2020) Structure, function, and regulation of the blood-brain barrier tight junction in central nervous system disorders. *Front Physiol.* **11**, 914, <https://doi.org/10.3389/fphys.2020.00914>
- 37 Zhang, J., Khvorostov, I., Hong, J.S., Oktay, Y., Vergnes, L., Nuebel, E. et al. (2016) UCP2 regulates energy metabolism and differentiation potential of human pluripotent stem cells. *EMBO J.* **35**, 899, <https://doi.org/10.15252/emj.201694054>
- 38 Rauf, A., Badoni, H., Abu-Izneid, T., Olatunde, A., Rahman, M.M., Painuli, S. et al. (2022) Neuroinflammatory markers: key indicators in the pathology of neurodegenerative diseases. *Molecules* **27**, <https://doi.org/10.3390/molecules27103194>
- 39 Wilson, 3rd, D.M., Cookson, M.R., Van Den Bosch, L., Zetterberg, H., Holtzman, D.M. and Dewachter, I. (2023) Hallmarks of neurodegenerative diseases. *Cell* **186**, 693–714
- 40 Boerma, R.S., Braun, K.P., van den Broek, M.P., van Berkestijn, F.M., Swinkels, M.E., Hagebeuk, E.O. et al. (2016) Remarkable phenytoin sensitivity in 4 children with SCN8A-related epilepsy: a molecular neuropharmacological approach. *Neurotherapeutics* **13**, 192–197, <https://doi.org/10.1007/s13311-015-0372-8>
- 41 Baker, E.M., Thompson, C.H., Hawkins, N.A., Wagnon, J.L., Wengert, E.R., Patel, M.K. et al. (2018) The novel sodium channel modulator GS-458967 (GS967) is an effective treatment in a mouse model of SCN8A encephalopathy. *Epilepsia* **59**, 1166–1176, <https://doi.org/10.1111/epi.14196>
- 42 Holmes, G.L. and Ben-Ari, Y. (2001) The neurobiology and consequences of epilepsy in the developing brain. *Pediatr. Res.* **49**, 320–325, <https://doi.org/10.1203/00006450-200103000-00004>
- 43 Ismail, F.Y., Fatemi, A. and Johnston, M.V. (2017) Cerebral plasticity: Windows of opportunity in the developing brain. *Eur. J. Paediatr. Neurol.* **21**, 23–48, <https://doi.org/10.1016/j.ejpn.2016.07.007>
- 44 Johnston, M.V., Ishida, A., Ishida, W.N., Matsushita, H.B., Nishimura, A. and Tsuji, M. (2009) Plasticity and injury in the developing brain. *Brain Dev.* **31**, 1–10, <https://doi.org/10.1016/j.braindev.2008.03.014>
- 45 Luo, J. (2022) TGF-beta as a key modulator of astrocyte reactivity: disease relevance and therapeutic implications. *Biomedicines* **10**, <https://doi.org/10.3390/biomedicines10051206>
- 46 Cacheaux, L.P., Ivens, S., David, Y., Lakhter, A.J., Bar-Klein, G., Shapira, M. et al. (2009) Transcriptome profiling reveals TGF-beta signaling involvement in epileptogenesis. *J. Neurosci.* **29**, 8927–8935, <https://doi.org/10.1523/JNEUROSCI.0430-09.2009>
- 47 Michetti, F., Clementi, M.E., Di Liddo, R., Valeriani, F., Ria, F., Rende, M. et al. (2023) The S100B protein: a multifaceted pathogenic factor more than a biomarker. *Int. J. Mol. Sci.* **24**, 9605–9620, <https://doi.org/10.3390/ijms24119605>
- 48 Singh, P. and Ali, S.A. (2022) Multifunctional role of S100 protein family in the immune system: an update. *Cells* **11**, 2274–2301, <https://doi.org/10.3390/cells11152274>
- 49 Jain, M., Singh, M.K., Shyam, H., Mishra, A., Kumar, S., Kumar, A. et al. (2021) Role of JAK/STAT in the neuroinflammation and its association with neurological disorders. *Ann. Neurosci.* **28**, 191–200, <https://doi.org/10.1177/09727531211070532>
- 50 Sun, H., Ma, D., Cheng, Y., Li, J., Zhang, W., Jiang, T. et al. (2023) The JAK-STAT signaling pathway in epilepsy. *Curr. Neuropharmacol.* **21**, 2049–2069, <https://doi.org/10.2174/1570159X21666221214170234>
- 51 Garcia-Mata, R., Boulter, E. and Burridge, K. (2011) The ‘invisible hand’: regulation of RHO GTPases by RHOGDIs. *Nat. Rev. Mol. Cell Biol.* **12**, 493–504, <https://doi.org/10.1038/nrm3153>
- 52 Mulherkar, S. and Tolia, K.F. (2020) RhoA-ROCK signaling as a therapeutic target in traumatic brain injury. *Cells* **9**, 245–257, <https://doi.org/10.3390/cells9010245>
- 53 Schmidt, S.I., Blaabjerg, M., Freude, K. and Meyer, M. (2022) RhoA signaling in neurodegenerative diseases. *Cells* **11**, 1520–1552, <https://doi.org/10.3390/cells11091520>
- 54 Gao, X. and Bayraktutan, U. (2023) TNF-alpha evokes blood-brain barrier dysfunction through activation of Rho-kinase and neurokinin 1 receptor. *Immunobiology* **228**, 152706, <https://doi.org/10.1016/j.imbio.2023.152706>

- 55 Yu, Y., Wu, Y., Wei, J., Huang, F., Mao, F., Nong, W. et al. (2022) NMDA mediates disruption of blood-brain barrier permeability via Rho/ROCK signaling pathway. *Neurochem. Int.* **154**, 105278, <https://doi.org/10.1016/j.neuint.2022.105278>
- 56 Xiao, Y., Zhang, Y., Yuan, W., Wang, C., Ge, Y., Huang, T. et al. (2024) Piezo2 contributes to traumatic brain injury by activating the RhoA/ROCK1 pathways. *Mol. Neurobiol.*, <https://doi.org/10.1007/s12035-024-04058-y>
- 57 Rodriguez-Gomez, J.A., Kavanagh, E., Engskog-Vlachos, P., Engskog, M.K.R., Herrera, A.J., Espinosa-Oliva, A.M. et al. (2020) Microglia: agents of the CNS pro-inflammatory response. *Cells* **9**, 1717–1759, <https://doi.org/10.3390/cells9071717>
- 58 Vizuete, A.F.K., Froes, F., Seady, M., Zanutto, C., Bobermin, L.D., Roginski, A.C. et al. (2022) Early effects of LPS-induced neuroinflammation on the rat hippocampal glycolytic pathway. *J. Neuroinflammation* **19**, 255, <https://doi.org/10.1186/s12974-022-02612-w>
- 59 Dai, S., Zheng, Y., Wang, Y. and Chen, Z. (2021) HMGB1, neuronal excitability and epilepsy. *Acta Epileptologica* **3**, 3–21, <https://doi.org/10.1186/s42494-021-00048-y>
- 60 Vezzani, A. (2014) Epilepsy and inflammation in the brain: overview and pathophysiology. *Epilepsy Curr.* **14**, 3–7, <https://doi.org/10.5698/1535-7511-14.s2.3>
- 61 Lopez-Colome, A.M., Lee-Rivera, I., Benavides-Hidalgo, R. and Lopez, E. (2017) Paxillin: a crossroad in pathological cell migration. *J. Hematol. Oncol.* **10**, 50, <https://doi.org/10.1186/s13045-017-0418-y>
- 62 Saikia, B.B., Bhowmick, S., Malat, A., Preetha Rani, M.R., Thaha, A. and Abdul-Muneer, P.M. (2024) ICAM-1 deletion using CRISPR/Cas9 protects the brain from traumatic brain injury-induced inflammatory leukocyte adhesion and transmigration cascades by attenuating the Paxillin/FAK-Dependent Rho GTPase Pathway. *J. Neurosci.* **44**, 1–17, <https://doi.org/10.1523/JNEUROSCI.1742-23.2024>
- 63 Stankiewicz, T.R. and Linseman, D.A. (2014) Rho family GTPases: key players in neuronal development, neuronal survival, and neurodegeneration. *Front Cell Neurosci.* **8**, 314, <https://doi.org/10.3389/fncel.2014.00314>
- 64 Guo, A.X., Cui, J.J., Wang, L.Y. and Yin, J.Y. (2020) The role of CSDE1 in translational reprogramming and human diseases. *Cell Commun. Signal.* **18**, 14, <https://doi.org/10.1186/s12964-019-0496-2>
- 65 Dong, R., Huang, R., Wang, J., Liu, H. and Xu, Z. (2021) Effects of microglial activation and polarization on brain injury after stroke. *Front Neurol.* **12**, 620948, <https://doi.org/10.3389/fneur.2021.620948>
- 66 Liu, J., Liu, L., Wang, X., Jiang, R., Bai, Q. and Wang, G. (2021) Microglia: a double-edged sword in intracerebral hemorrhage from basic mechanisms to clinical research. *Front Immunol.* **12**, 675660, <https://doi.org/10.3389/fimmu.2021.675660>
- 67 van Loo, G. and Bertrand, M.J.M. (2023) Death by TNF: a road to inflammation. *Nat. Rev. Immunol.* **23**, 289–303, <https://doi.org/10.1038/s41577-022-00792-3>
- 68 Chen, H.C., Chang, W.C., Chuang, J.Y., Chang, K.Y., Liou, J.P. and Hsu, T.I. (2023) The complex role of eicosanoids in the brain: Implications for brain tumor development and therapeutic opportunities. *Biochim. Biophys. Acta Rev. Cancer* **1878**, 188957, <https://doi.org/10.1016/j.bbcan.2023.188957>
- 69 Liu, X., Davis, C.M. and Alkayed, N.J. (2018) Eicosanoids and reactive oxygen species interplay in brain injury and neuroprotection. *Antioxid Redox Signal.* **28**, 987–1007, P450, <https://doi.org/10.1089/ars.2017.7056>
- 70 Mancini, C., Gohlke, S., Garcia-Carrizo, F., Zagoriy, V., Stephanowitz, H. and Schulz, T.J. (2021) Identification of biomarkers of brown adipose tissue aging highlights the role of dysfunctional energy and nucleotide metabolism pathways. *Sci. Rep.* **11**, 19928, <https://doi.org/10.1038/s41598-021-99362-1>
- 71 Borowicz-Reutt, K.K. and Czuczwar, S.J. (2020) Role of oxidative stress in epileptogenesis and potential implications for therapy. *Pharmacol. Rep.* **72**, 1218–1226, <https://doi.org/10.1007/s43440-020-00143-w>
- 72 Guo, C., Sun, L., Chen, X. and Zhang, D. (2013) Oxidative stress, mitochondrial damage and neurodegenerative diseases. *Neural Regen. Res.* **8**, 2003–2014
- 73 Wang, M., Gui, X., Wu, L., Tian, S., Wang, H., Xie, L. et al. (2020) Amino acid metabolism, lipid metabolism, and oxidative stress are associated with post-stroke depression: a metabolomics study. *BMC Neurol.* **20**, 250, <https://doi.org/10.1186/s12883-020-01780-7>
- 74 Manczak, M., Jung, Y., Park, B.S., Partovi, D. and Reddy, P.H. (2005) Time-course of mitochondrial gene expressions in mice brains: implications for mitochondrial dysfunction, oxidative damage, and cytochrome c in aging. *J. Neurochem.* **92**, 494–504, <https://doi.org/10.1111/j.1471-4159.2004.02884.x>
- 75 Onyango, I.G., Lu, J., Rodova, M., Lezi, E., Crafter, A.B. and Swerdlow, R.H. (2010) Regulation of neuron mitochondrial biogenesis and relevance to brain health. *Biochim. Biophys. Acta* **1802**, 228–234, <https://doi.org/10.1016/j.bbadis.2009.07.014>
- 76 Popay, T.M., Wang, J., Adams, C.M., Howard, G.C., Codreanu, S.G., Sherrod, S.D. et al. (2021) MYC regulates ribosome biogenesis and mitochondrial gene expression programs through its interaction with host cell factor-1. *Elife* **10**, 1–39, <https://doi.org/10.7554/eLife.60191>
- 77 Qi, X. (2017) eIF2alpha links mitochondrial dysfunction to dendritic degeneration. *J. Cell Biol.* **216**, 555–557, <https://doi.org/10.1083/jcb.201701062>
- 78 Wang, X. and Proud, C.G. (2022) The role of eIF2 phosphorylation in cell and organismal physiology: new roles for well-known actors. *Biochem. J.* **479**, 1059–1082, <https://doi.org/10.1042/BCJ20220068>
- 79 Bjorkman, S. and Oliveira Pereira, R. (2021) The interplay between mitochondrial reactive oxygen species, endoplasmic reticulum stress, and Nrf2 signaling in cardiometabolic health. *Antioxid Redox Signal.* **35**, 252–269, <https://doi.org/10.1089/ars.2020.8220>
- 80 Bouras, M., Asehounne, K. and Roquilly, A. (2022) Immune modulation after traumatic brain injury. *Front Med. (Lausanne)* **9**, 995044, <https://doi.org/10.3389/fmed.2022.995044>
- 81 Clark, D.N., Begg, L.R. and Filiano, A.J. (2022) Unique aspects of IFN-gamma/STAT1 signaling in neurons. *Immunol. Rev.* **311**, 187–204, <https://doi.org/10.1111/imr.13092>
- 82 Wang, Z. and Chen, G. (2023) Immune regulation in neurovascular units after traumatic brain injury. *Neurobiol. Dis.* **179**, 106060, <https://doi.org/10.1016/j.nbd.2023.106060>
- 83 Liston, A., Dooley, J. and Yshii, L. (2022) Brain-resident regulatory T cells and their role in health and disease. *Immunol. Lett.* **248**, 26–30, <https://doi.org/10.1016/j.imlet.2022.06.005>

- 84 Liu, R., Li, Y., Wang, Z., Chen, P., Xie, Y., Qu, W. et al. (2023) Regulatory T cells promote functional recovery after spinal cord injury by alleviating microglia inflammation via STAT3 inhibition. *CNS Neurosci. Ther.* **29**, 2129–2144, <https://doi.org/10.1111/cns.14161>
- 85 Ito, M., Komai, K., Mise-Omata, S., Iizuka-Koga, M., Noguchi, Y., Kondo, T. et al. (2019) Brain regulatory T cells suppress astrogliosis and potentiate neurological recovery. *Nature* **565**, 246–250, <https://doi.org/10.1038/s41586-018-0824-5>
- 86 Kramer, T.J., Hack, N., Bruhl, T.J., Menzel, L., Hummel, R., Griemert, E.V. et al. (2019) Depletion of regulatory T cells increases T cell brain infiltration, reactive astrogliosis, and interferon-gamma gene expression in acute experimental traumatic brain injury. *J. Neuroinflammation* **16**, 163, <https://doi.org/10.1186/s12974-019-1550-0>
- 87 Yue, J., Xu, R., Yin, C., Yang, H., Zhang, C. and Zhao, D. (2022) Negative effects of brain regulatory T cells depletion on epilepsy. *Prog. Neurobiol.* **217**, 102335, <https://doi.org/10.1016/j.pneurobio.2022.102335>
- 88 Ronaldson, P.T. and Davis, T.P. (2020) Regulation of blood-brain barrier integrity by microglia in health and disease: a therapeutic opportunity. *J. Cereb. Blood Flow Metab.* **40**, S6–S24, <https://doi.org/10.1177/0271678X20951995>
- 89 Vezzani, A., Balosso, S. and Ravizza, T. (2019) Neuroinflammatory pathways as treatment targets and biomarkers in epilepsy. *Nat. Rev. Neurol.* **15**, 459–472, <https://doi.org/10.1038/s41582-019-0217-x>
- 90 Bild, W., Vasincu, A., Rusu, R.N., Ababei, D.C., Stana, A.B., Stanciu, G.D. et al. (2022) Impact of the renin-angiotensin system on the pathogeny and pharmacotherapeutics of neurodegenerative diseases. *Biomolecules* **12**, 1429–1459, <https://doi.org/10.3390/biom12101429>
- 91 Mowry, F.E., Peaden, S.C., Stern, J.E. and Biancardi, V.C. (2021) TLR4 and AT1R mediate blood-brain barrier disruption, neuroinflammation, and autonomic dysfunction in spontaneously hypertensive rats. *Pharmacol. Res.* **174**, 105877, <https://doi.org/10.1016/j.phrs.2021.105877>
- 92 Villapol, S. and Saavedra, J.M. (2015) Neuroprotective effects of angiotensin receptor blockers. *Am. J. Hypertens.* **28**, 289–299, <https://doi.org/10.1093/ajh/hpu197>
- 93 Yasar, S. (2022) Candesartan—the next anti-amyloid drug? *Brain Commun.* **4**, fcac293, <https://doi.org/10.1093/braincomms/fcac293>
- 94 Arganaraz, G.A., Konno, A.C., Perosa, S.R., Santiago, J.F., Boim, M.A., Vidotti, D.B. et al. (2008) The renin-angiotensin system is upregulated in the cortex and hippocampus of patients with temporal lobe epilepsy related to mesial temporal sclerosis. *Epilepsia* **49**, 1348–1357, <https://doi.org/10.1111/j.1528-1167.2008.01581.x>
- 95 Gomes, K.P., Braga, P.P.P., de Lima, C.Q., Ghazale, P.P., Pedrino, G.R., Mendes, E.P. et al. (2020) Antiepileptic effects of long-term intracerebroventricular infusion of angiotensin-(1-7) in an animal model of temporal lobe epilepsy. *Clin. Sci. (Lond.)* **134**, 2263–2277, <https://doi.org/10.1042/CS20200514>
- 96 Gouveia, T.L., Frangiotti, M.I., de Brito, J.M., de Castro Neto, E.F., Sakata, M.M., Febba, A.C. et al. (2012) The levels of renin-angiotensin related components are modified in the hippocampus of rats submitted to pilocarpine model of epilepsy. *Neurochem. Int.* **61**, 54–62, <https://doi.org/10.1016/j.neuint.2012.04.012>
- 97 Ramos, A.J. (2021) Brain angiotensin system: a new promise in the management of epilepsy? *Clin. Sci. (Lond.)* **135**, 725–730, <https://doi.org/10.1042/CS20201296>
- 98 Wang, X., Khaidakov, M., Ding, Z., Mitra, S., Lu, J., Liu, S. et al. (2012) Cross-talk between inflammation and angiotensin II: studies based on direct transfection of cardiomyocytes with AT1R and AT2R cDNA. *Exp. Biol. Med. (Maywood)* **237**, 1394–1401, <https://doi.org/10.1258/ebm.2012.012212>
- 99 Park, H.S., You, M.J., Yang, B., Jang, K.B., Yoo, J., Choi, H.J. et al. (2020) Chronically infused angiotensin II induces depressive-like behavior via microglia activation. *Sci. Rep.* **10**, 22082, <https://doi.org/10.1038/s41598-020-79096-2>
- 100 Zolezzi, J.M., Santos, M.J., Bastias-Candia, S., Pinto, C., Godoy, J.A. and Inestrosa, N.C. (2017) PPARs in the central nervous system: roles in neurodegeneration and neuroinflammation. *Biol. Rev. Camb. Philos. Soc.* **92**, 2046–2069, <https://doi.org/10.1111/brv.12320>
- 101 Corona, J.C. and Duchen, M.R. (2016) PPARgamma as a therapeutic target to rescue mitochondrial function in neurological disease. *Free Radic. Biol. Med.* **100**, 153–163, <https://doi.org/10.1016/j.freeradbiomed.2016.06.023>
- 102 Friedman, A., Bar-Klein, G., Serlin, Y., Parment, Y., Heinemann, U. and Kaufer, D. (2014) Should losartan be administered following brain injury? *Expert Rev. Neurother.* **14**, 1365–1375, <https://doi.org/10.1586/14737175.2014.972945>
- 103 Hong, S., JianCheng, H., JiaWen, W., ShuQin, Z., GuiLian, Z., HaiQin, W. et al. (2019) Losartan inhibits development of spontaneous recurrent seizures by preventing astrocyte activation and attenuating blood-brain barrier permeability following pilocarpine-induced status epilepticus. *Brain Res. Bull.* **149**, 251–259, <https://doi.org/10.1016/j.brainresbull.2019.05.002>
- 104 Liang, L., Yuan, W., Qu, L., Li, H., Zhang, L., Fan, G.C. et al. (2019) Administration of losartan preserves cardiomyocyte size and prevents myocardial dysfunction in tail-suspended mice by inhibiting p47(phox) phosphorylation, NADPH oxidase activation and MuRF1 expression. *J. Transl. Med.* **17**, 279, <https://doi.org/10.1186/s12967-019-2021-1>
- 105 Nguyen Dinh Cat, A., Montezano, A.C., Burger, D. and Touyz, R.M. (2013) Angiotensin II, NADPH oxidase, and redox signaling in the vasculature. *Antioxid Redox Signal.* **19**, 1110–1120, <https://doi.org/10.1089/ars.2012.4641>
- 106 Hanael, E., Chai, O., Konstantin, L., Gibeon, L., Rapaport, K., Ruggeri, M. et al. (2022) Telmisartan as an add-on treatment for dogs with refractory idiopathic epilepsy: a nonrandomized, uncontrolled, open-label clinical trial. *J. Am. Vet. Med. Assoc.* **260**, 735–740, <https://doi.org/10.2460/javma.20.12.0683>
- 107 Quinlan, S., Merino-Serrais, P., Di Grande, A., Dussmann, H., Prehn, J.H.M., Ni Chonghaile, T. et al. (2019) The anti-inflammatory compound candesartan cilexetil improves neurological outcomes in a mouse model of neonatal hypoxia. *Front Immunol.* **10**, 1752, <https://doi.org/10.3389/fimmu.2019.01752>
- 108 Goel, R., Bhat, S.A., Hanif, K., Nath, C. and Shukla, R. (2018) Angiotensin II receptor blockers attenuate lipopolysaccharide-induced memory impairment by modulation of NF-kappaB-mediated BDNF/CREB expression and apoptosis in spontaneously hypertensive rats. *Mol. Neurobiol.* **55**, 1725–1739, <https://doi.org/10.1007/s12035-017-0450-5>
- 109 Gong, Y. and Hewett, J.A. (2018) Maintenance of the innate seizure threshold by cyclooxygenase-2 is not influenced by the translational silencer, t-cell intracellular antigen-1. *Neuroscience* **373**, 37–51, <https://doi.org/10.1016/j.neuroscience.2018.01.004>

- 110 Hickey, R.W., Adelson, P.D., Johnnides, M.J., Davis, D.S., Yu, Z., Rose, M.E. et al. (2007) Cyclooxygenase-2 activity following traumatic brain injury in the developing rat. *Pediatr. Res.* **62**, 271–276, <https://doi.org/10.1203/PDR.0b013e3180db2902>
- 111 Huang, C., Santofimia-Castano, P. and Iovanna, J. (2021) NUPR1: a critical regulator of the antioxidant system. *Cancers (Basel)* **13**, 3670–3684, <https://doi.org/10.3390/cancers13153670>
- 112 Chen, J., He, W., Hu, X., Shen, Y., Cao, J., Wei, Z. et al. (2017) A role for ErbB signaling in the induction of reactive astrogliosis. *Cell Discov.* **3**, 17044, <https://doi.org/10.1038/celldisc.2017.44>
- 113 Doege, C., Luedde, M. and Kostev, K. (2023) Association between use of angiotensin receptor blockers and incidence of epilepsy in patients with hypertension-reply. *JAMA Neurol.* **80**, 532–533, <https://doi.org/10.1001/jamaneurol.2023.0407>
- 114 Wen, X., Otoo, M.N., Tang, J., Brothers, T., Ward, K.E., Asal, N. et al. (2024) Angiotensin receptor blockers for hypertension and risk of epilepsy. *JAMA Neurol.* **81**, 866–874, <https://doi.org/10.1001/jamaneurol.2024.1714>
- 115 Bulsara, K.G. and Makaryus, A.N. (2024) *Candesartan*, StatPearls, Treasure Island (FL)
- 116 Hill, S.F., Yu, W., Ziobro, J., Chalasani, S., Reger, F. and Meisler, M.H. (2024) Long-term downregulation of the sodium channel gene *Scn8a* is therapeutic in mouse models of SCN8A epilepsy. *Ann. Neurol.* **95**, 754–759, <https://doi.org/10.1002/ana.26861>
- 117 Klein, P., Friedman, A., Hameed, M.Q., Kaminski, R.M., Bar-Klein, G., Klitgaard, H. et al. (2020) Repurposed molecules for antiepileptogenesis: Missing an opportunity to prevent epilepsy? *Epilepsia* **61**, 359–386, <https://doi.org/10.1111/epi.16450>
- 118 Huang, L., Nakamura, Y., Lo, E.H. and Hayakawa, K. (2019) Astrocyte signaling in the neurovascular unit after central nervous system injury. *Int. J. Mol. Sci.* **20**, 282–296, <https://doi.org/10.3390/ijms20020282>
- 119 McKee, C.A. and Lukens, J.R. (2016) Emerging roles for the immune system in traumatic brain injury. *Front Immunol.* **7**, 556, <https://doi.org/10.3389/fimmu.2016.00556>
- 120 Simon, D.W., McGeachy, M.J., Bayir, H., Clark, R.S.B., Loane, D.J. and Kochanek, P.M. (2017) The far-reaching scope of neuroinflammation after traumatic brain injury. *Nat. Rev. Neurol.* **13**, 572, <https://doi.org/10.1038/nrneurol.2017.116>
- 121 Nguyen, T.M., Shafi, A., Nguyen, T. and Draghici, S. (2019) Identifying significantly impacted pathways: a comprehensive review and assessment. *Genome Biol.* **20**, 203, <https://doi.org/10.1186/s13059-019-1790-4>